ISOLDE Nuclear Reaction and Nuclear Structure Course[1]

Lecture notes on

"Quantum scattering theory and direct nuclear reactions"

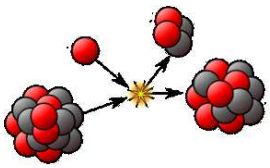

Antonio M. Moro Muñoz (moro@us.es)

Departamento de Física Atómica, Molecular y Nuclear
Universidad de Sevilla, Spain

[1] Course held at ISOLDE, April 22th–25th 2014

Contents

Chapter 1

Some general scattering theory

1.1 Introduction

Most of our present knowledge of stable and exotic nuclei stems from the analysis of nuclear reactions. These processes are traditionally separated into two groups: compound nucleus and direct reactions. In these notes, we will be concerned only with the latter. These refer to collisions in which the nuclei make "glancing" contact and separate immediately. They are said also to be peripheral (surface) processes. The colliding nuclei preserve their "identity" ($a + A \rightarrow a^* + A^*$). Thus, these processes involve a small number of degrees of freedom and can be characterized and studied in terms of the excitation of these degrees of freedom.

The final goal of the scattering theory is to develop appropriate models to which compare the measured observables, with the aim of extracting information on the structure of the colliding nuclei as well as understanding the dynamics governing these processes. The measured quantities are typically total or partial cross sections with respect to angle and/or energy of the outgoing nuclei. Therefore, the challenge of reaction theory is to obtain these cross sections by solving the dynamical equations of the system (at non-relativistic energies, the Schrödinger equation) with a realistic but amenable structure model of the colliding nuclei. By solving the Schrödinger equation, one obtains the wavefunction of the system. This wavefunction will be a function of the degrees of freedom (eg. internal coordinates) of the projectile and target, denoted generically as ξ_p and ξ_t, as well as on the relative coordinate between them ($\mathbf{R}$). Thus, we will express the total wavefunction as $\Psi(\mathbf{R}, \xi_p, \xi_t)$. The Hamiltonian of the system is written in the form

$$H = \hat{T}_{\mathbf{R}} + H_p(\xi_p) + H_t(\xi_t) + V(\mathbf{R}, \xi_p, \xi_t), \tag{1.1}$$

where $\hat{T}_{\mathbf{R}}$ is the kinetic energy operator ($\hat{T} = -\frac{\hbar^2}{2\mu}\nabla^2_{\mathbf{R}}$) and $H_p(\xi_p)$ ($H_t(\xi_t)$) denote the projectile (target) internal Hamiltonians and $V(\mathbf{R}, \xi_p, \xi_t)$ is the projectile-target interaction. After the collision, the projectile and target may exchange some nucleons, or even breakup, so the Hamiltonian (1.1) corresponds actually to the entrance channel. To denote the possible mass partitions that may arise in a reaction, we will use greek letters,

with α denoting the initial partition. So, the previous Hamiltonian is rewritten as

$$H = \hat{T}_\alpha + H_\alpha(\xi_\alpha) + V_\alpha(\mathbf{R}_\alpha, \xi_\alpha) \tag{1.2}$$

where ξ_α denotes the projectile and target internal coordinates in partition α. The total energy of the system is given by the sum of the kinetic energy (E_α) and the internal energy of the projectile and target:

$$E = E_\alpha + \varepsilon_\alpha = \frac{\hbar^2 {K_\alpha}^2}{2\mu_\alpha} + \varepsilon_\alpha \ , \tag{1.3}$$

where $\hbar\mathbf{K}_\alpha$ is just the linear momentum. The wavefunction $\Psi(\mathbf{R}, \xi)$ will be a solution of the time dependent Schrödinger equation. For the purpose of extracting the scattering observables, one may solve the time-independent Schrödinger equation for a total energy E (see Chapter 1 of [6] for a discussion on the relation between the time-dependent and time-independent pictures). So, $\Psi_{\mathbf{K}}$ will be a solution of

$$[H - E]\, \Psi_{\mathbf{K}} = 0 \ . \tag{1.4}$$

This is a second order differential equation that must be solved subject to the appropriate boundary conditions. These boundary conditions must reflect the nature of a scattering process. In our time-independent picture, the incident beam will be represented by a plane wave[1]. After the collision with the target, a set of outgoing spherical waves will be formed. The situation is schematically depicted in Fig. 1.1. So, asymptotically,

$$\Psi^{(+)}_{\mathbf{K}_0}(\mathbf{R}, \xi) \to \Phi_0(\xi) e^{i\mathbf{K}_0 \cdot \mathbf{R}} \ + \ \text{outgoing spherical waves}, \tag{1.5}$$

with $\Phi_0(\xi) \equiv \phi_p^{(0)}(\xi_p)\phi_t^{(0)}(\xi_t)$ and where the superscript "+" indicates that we this corresponds to the solution with outgoing boundary conditions (mathematically, one may construct also the solution with incoming boundary conditions).

During the collision, the incident wave will be highly distorted by the projectile–target interaction but, after the collision, at sufficiently large distances (that is, when V becomes negligible), the projectile and target will energy in any of the (kinematically allowed) eigenstates of system. So, asymptotically, we may write[2]

$$\begin{aligned}
\Psi^{(+)}_{\mathbf{K}_\alpha} \to \Phi_\alpha(\xi_\alpha) e^{i\mathbf{K}_\alpha \cdot \mathbf{R}_\alpha} + \Phi_\alpha(\xi_\alpha) f_{\alpha,\alpha}(\theta) \frac{e^{iK_\alpha R_\alpha}}{R_\alpha} \\
+ \sum_{\alpha' \neq \alpha} \Phi_{\alpha'}(\xi_\alpha) f_{\alpha',\alpha}(\theta) \frac{e^{iK_{\alpha'} R_\alpha}}{R_\alpha} \\
+ \sum_{\beta} \Phi_\beta(\xi_\beta) f_{\beta,\alpha}(\theta) \frac{e^{iK_\beta R_\beta}}{R_\beta},
\end{aligned} \tag{1.6}$$

[1] This is only true for the case of short-range potentials; in presence of the Coulomb potential, the incident wavefunction is represented by a Coulomb wave

[2] Note that we distinguish between R_α and R_β since, for a rearrangement process, the coordinates will be different. We will return to this issue in Chapter 4.

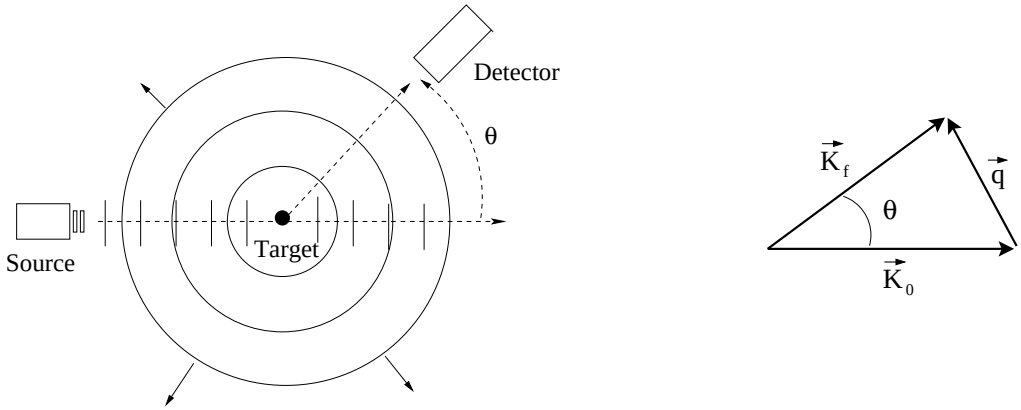

Figure 1.1: Left: schematic representation of a scattering process. Right: initial, final and transferred momenta.

The first, second and third lines correspond to elastic, inelastic and transfer channels, respectively. The angle θ is the CM scattering angle, and corresponds to the angle between the incident and final momenta ($\mathbf{K}_\alpha$ and $\mathbf{K}_\beta$). The function $e^{iK_\beta R_\beta}/R_\beta$ is a spherical outgoing wave. The function multiplying this outgoing wave is the *scattering amplitude* for channel β. Note (Fig. 1.1) that the vectors $\mathbf{K}_\beta$ and $\mathbf{R}_\beta$ are parallel. The *differential cross section* for particles scattering in the direction θ in channel β is defined as the *flux of scattered particles through the area $dA = r^2 d\Omega$ in the direction θ, per unit incident flux.* This quantity is directly related to the scattering amplitude as (see e.g. Chap. 3, Sec. G of [11])

$$\left(\frac{d\sigma}{d\Omega}\right)_{\alpha\to\beta} = \frac{v_\beta}{v_\alpha}\left|f_{\beta,\alpha}(\theta)\right|^2 . \tag{1.7}$$

It is customary to define the transition matrix (T-matrix):

$$\mathcal{T}_{\beta\alpha}(\theta) = -\frac{2\pi\hbar^2}{\mu_\beta} f_{\beta\alpha}(\theta) \ , \tag{1.8}$$

in terms of which

$$\left(\frac{d\sigma}{d\Omega}\right)_{\alpha\to\beta} = \frac{\mu_\alpha\mu_\beta}{(2\pi\hbar^2)^2}\left|\frac{K_\beta}{K_\alpha}\mathcal{T}_{\beta\alpha}(\theta)\right|^2 \tag{1.9}$$

1.2 An integral equation for $f_{\beta,\alpha}(\theta)$

Consider that we are interested on a particular channel β. The scattering amplitude corresponding to this particular channel can be obtained from the asymptotic form of the total wavefunction, Eq. (1.6), multiplying on the left by the "internal" wavefunction $\Phi^*_\beta(\xi_\beta)$ corresponding the channel of interest, and integrating over the coordinates ξ_β, i.e.

$$(\Phi_\beta|\Psi^{(+)}_{\mathbf{K}_\alpha}\rangle \xrightarrow{R\gg} \delta_{\beta,\alpha}e^{i\mathbf{K}_\alpha\cdot\mathbf{R}_\alpha} + f_{\beta,\alpha}(\theta)\frac{e^{iK_\beta R_\beta}}{R_\beta} \tag{1.10}$$

where $(\ldots\rangle$ denotes integration over internal coordinates only. Thus, $(\Phi_\beta|\Psi^{(+)}_{\mathbf{K}_\alpha}\rangle$ remains a function of $\mathbf{R}_\beta$, so we may define $X_\beta(\mathbf{R}_\beta) \equiv (\Phi_\beta|\Psi^{(+)}_{\mathbf{K}_\alpha}\rangle$. So, if we know $\Psi^{(+)}_{\mathbf{K}_\alpha}$ or an approximation to it, we can extract the scattering amplitude from the asymptotics of $X_\beta(\mathbf{R}_\beta)$. Using this result, it is possible to obtain a formal expression for $f_{\beta,\alpha}(\theta)$. We start writing the Schrödinger equation, using the form of the Hamiltonian appropriate for the channel β, that is,

$$H = \hat{T}_\beta + H_\beta(\xi_\beta) + V_\beta(\mathbf{R}_\beta) \tag{1.11}$$

Using this form of the Hamiltonian in the Schrödinger equation, Eq. (1.4), multiplying on the left by $\Phi^*_\beta(\xi_\beta)$ and integrating along the coordinates ξ_β we get the *projected* equation:

$$[\hat{T}_\beta + \varepsilon_\beta - E]X_\beta(\mathbf{R}_\beta) = -(\Phi_\beta|V_\beta\Psi^{(+)}_{\mathbf{K}_\alpha}\rangle \tag{1.12}$$

were we have used $\varepsilon_\beta = \langle\Phi_\beta(\xi_\beta)|H_\beta|\Phi_\beta(\xi_\beta)\rangle$ and the fact that the kinetic energy operator does not depend on the internal coordinates ξ_β. This is a second-order inhomogeneous differential equation for the function X_β. The most general solution is the sum of the solution of the corresponding homogeneous equation, plus a particular solution of the inhomogeneous equation. The homogeneous equation is trivially solved, since it contains only the kinetic energy operator; its solution is just a plane wave with momentum $\mathbf{K}_\beta$, with modulus $K_\beta = \sqrt{2\mu_\beta(E-\varepsilon_\beta)}/\hbar$. The particular solution of the inhomogeneous equation can be formally obtained using Green function techniques (see, for example, [21, 11]) leading to:

$$X_\beta(\mathbf{R}_\beta) = e^{i\mathbf{K}_\alpha\cdot\mathbf{R}_\alpha}\delta_{\alpha,\beta} - \frac{\mu_\beta}{2\pi\hbar^2}\int G_\beta(\mathbf{R}_\beta,\mathbf{R}'_\beta)(\Phi_\beta|V_\beta\Psi^{(+)}_\alpha\rangle d\mathbf{R}'_\beta \tag{1.13}$$

where G_β is the Green function in channel β. Explicitly:

$$G_\beta(\mathbf{R}_\beta,\mathbf{R}'_\beta) = \frac{e^{iK_\beta|\mathbf{R}_\beta-\mathbf{R}'_\beta|}}{|\mathbf{R}_\beta-\mathbf{R}'_\beta|} \tag{1.14}$$

To extract the scattering amplitude, we must take the asymptotic limit, $R_\beta \gg R'_\beta$. In this limit, the Green function reduces to[3]

$$G_\beta(\mathbf{R}_\beta,\mathbf{R}'_\beta) \to \frac{e^{iK_\beta R_\beta}}{R_\beta} \tag{1.15}$$

and the function $X_\beta(\mathbf{R}_\beta)$ tends to

$$X_\beta(\mathbf{R}_\beta) \xrightarrow{R_\beta\gg} e^{i\mathbf{K}_\alpha\cdot\mathbf{R}_\alpha}\delta_{\alpha,\beta} - \frac{\mu_\beta}{2\pi\hbar^2}\frac{e^{iK_\beta R_\beta}}{R_\beta}(\Phi_\beta|V_\beta\Psi^{(+)}_{\mathbf{K}_\alpha}\rangle \tag{1.16}$$

Comparing with the asymptotic form (1.6), and recalling the definition of the scattering amplitude, we have

$$\begin{aligned} f_{\beta,\alpha}(\theta) &= -\frac{\mu_\beta}{2\pi\hbar^2}\langle e^{-i\mathbf{K}_\beta\mathbf{R}_\beta}\Phi_\beta|V_\beta\Psi^{(+)}_{\mathbf{K}_\alpha}\rangle \\ &= -\frac{\mu_\beta}{2\pi\hbar^2}\int\int e^{-i\mathbf{K}_\beta\mathbf{R}_\beta}\Phi^*_\beta(\xi_\beta)V_\beta(\mathbf{R}_\beta,\xi_\beta)\Psi^{(+)}_{\mathbf{K}_\alpha}d\xi_\beta d\mathbf{R}_\beta \end{aligned} \tag{1.17}$$

[3]For $R_\beta \gg R'_\beta$, $|\mathbf{R}_\beta - \mathbf{R}'_\beta| \approx R_\beta - \hat{R}_\beta\cdot\hat{R}'_\beta = \hat{K}_\beta\cdot\hat{R}'_\beta$.

Or, in terms of the T-matrix,

$$\boxed{\mathcal{T}_{\beta,\alpha} = \int\int e^{-i\mathbf{K}_\beta \mathbf{R}_\beta} \Phi^*_\beta(\xi_\beta) V_\beta(\mathbf{R}_\beta, \xi_\beta) \Psi^{(+)}_{\mathbf{K}_\alpha}(\mathbf{R}_\alpha, \xi_\alpha) d\xi_\beta d\mathbf{R}_\beta.} \tag{1.18}$$

1.3 Gell-Mann–Goldberger transformation (two-potential formula)

A more general expression for Eq. (1.18) can found introducing an auxiliary (and by now arbitrary) potential $U_\beta(\mathbf{R}_\beta)$ on both sides of Eq. (1.12),

$$[\hat{T}_\beta + U_\beta + \varepsilon_\beta - E] X_\beta(\mathbf{R}_\beta) = -(\Phi_\beta | V_\beta - U_\beta \Psi^{(+)}_{\mathbf{K}_\alpha}\rangle \tag{1.19}$$

where, again, $X_\beta(\mathbf{R}_\beta) \equiv (\Phi_\beta | \Psi^{(+)}_{\mathbf{K}_\alpha}\rangle$.

The solution of (1.19) is given by a general solution of the homogeneous equation, plus a particular solution of the full equation. The homogeneous equation is given by

$$[\hat{T}_\beta + U_\beta + \varepsilon_\beta - E] \chi^+_\beta(\mathbf{R}_\beta) = 0 \tag{1.20}$$

This equation represents the scattering of the particles in channel β under the potential U_β. The solution is of the form

$$\chi^{(+)}_\beta(\mathbf{R}_\beta) = e^{i\mathbf{K}_\beta \cdot \mathbf{R}_\beta} + \text{outgoing spherical waves} \tag{1.21}$$

In the next chapter, we will discuss in more detail how this equation is solved in practical situations, making use of the partial wave expansion.

Finally, the full equation (1.19) is solved adding a particular solution of the inhomogeneous equation. This is done using again Green function techniques. Details are given in [6]. The full solution (which generalizes Eq. (1.16)) is written as

$$X_\beta(\mathbf{R}_\beta) \equiv (\Phi_\beta | \Psi^{(+)}_{\mathbf{K}_\alpha}\rangle = \chi^+_\beta(\mathbf{R}_\beta)\delta_{\alpha\beta} + \int G^{(+)}_\beta(\mathbf{R}_\beta, \mathbf{R}'_\beta)(\Phi_\beta | V_\beta - U_\beta \Psi^{(+)}_{\mathbf{K}_\alpha} d\mathbf{R}'_\beta \tag{1.22}$$

The scattering amplitude (or the T-matrix) is extracted from the asymptotics of the outgoing waves. Nnote that, we have outgoing waves in both terms of the RHS of the previous equation, and giving rise also to two contributions to the scattering amplitude,

$$\boxed{\mathcal{T}_{\beta,\alpha} = \mathcal{T}^{(0)}_{\beta,\alpha}\delta_{\alpha\beta} + \int\int \chi^{(-)*}_\beta(\mathbf{K}_\beta, \mathbf{R}_\beta) \Phi_\beta(\xi_\beta)[V_\beta - U_\beta] \Psi^{(+)}_{\mathbf{K}_\alpha} d\xi_\beta d\mathbf{R}_\beta,} \tag{1.23}$$

The first term is the scattering amplitude due to the potential U_β and is present only for the channel $\beta = \alpha$. In here, $\chi^{(-)}_\beta$, is the time-reverse of $\chi^{(+)}$ and corresponds to the solution consisting on a plane wave with momentum $\mathbf{K}_\beta$ and ingoing spherical waves. It can be readily obtained from $\chi^{(+)}$ using the relationship $\chi^{(-)*}(\mathbf{K}, \mathbf{R}) = \chi^{(+)}(-\mathbf{K}, \mathbf{R})$.

The result (1.23) is known as the **Gell-Mann–Goldberger transformation** or **two-potential formula**. This expression is exact but it cannot be solved as such, since it contains the exact wavefunction of the system. However, it provides a very useful starting point to derive approximate expressions, as we will see later on.

1.4 Defining the modelspace

We have seen that the dynamics of the system in a scattering process is encoded in the full wavefunction, $\Psi^{(+)}$. Formally, it can be obtained by solving the Schrödinger equation of the system. Asymptotically, this wavefunction consists on an incoming plane plane, and outgoing spherical waves in all possible channels. Practical calculations require as a first step reducing the full space to a tractable modelspace. This is motivated by two things: (i) the channels of interest to analyze a particular experiment and (ii) the numerical/computational complexity of the problem. For example, if we are interested in analyzing some inelastic scattering experiment, our model space might consist on the ground state of the projectile and target, plus the states more strongly populated in the experiment.

The formal procedure to reduce the problem from the full space to a selected modelspace was developed by Feshbach [9, 10]. The idea is to separate the full space into two parts, denoted as P and Q. The P space comprise the channels of interest and will therefore be taken into account explicitly in the model wavefunction $\Psi^{(+)}$. The Q space is composed by the remaining channels. So, following Feshbach (see also [6] and [11], Chapter 8G), we may write $\Psi^{(+)} = \Psi_P + \Psi_Q$. The components Ψ_P and Ψ_Q obey a complicated system coupled equations, with the deceptively simple form

$$(E - H_{PP})\Psi_P = H_{PQ}\Psi_Q \tag{1.24}$$

$$(E - H_{QQ})\Psi_Q = H_{QP}\Psi_P \tag{1.25}$$

where $H_{PP} = PHP$, $H_{PQ} = PHQ$, and so on. The projected Hamiltonian H_{PP} contains the coupling among the states of the P space, and likewise for H_{QQ}. The terms H_{PQ} and H_{QP} describe couplings between the states of P and those of Q. Since we are interested only in Ψ_P, we eliminate Ψ_Q from the RHS of the first equation, using the second equation:

$$\left[E - H_{PP} - H_{PQ}\frac{1}{E - H_{QQ} + i\epsilon}H_{QP}\right]\Psi_P = 0 \tag{1.26}$$

Let us rewrite this equation as

$$\left[E - H_\alpha - T_\alpha - \mathcal{V}\right]\Psi_P = 0 \tag{1.27}$$

with

$$\mathcal{V} = V_{PP} + V_{PQ}\frac{1}{E - H_{QQ} + i\epsilon}V_{QP} \tag{1.28}$$

Direct reaction theories replace the above equation by an approximated one of the form

$$(E - H_{\text{eff}})\Psi_{\text{model}} = 0 \tag{1.29}$$

where H_{eff} is an effective Hamiltonian which aims at representing the complicated object $\mathcal{V}$. Although the Feshbach formalism provides a expression for such operator, it cannot be evaluated in practice. Yet, this formal solution provides an useful guidance on how to

replace such a complicated object by some approximate one. In particular, the effective Hamiltonian is found to be complex, energy-dependent and non-local. Furthermore, since the effective Hamiltonian involves the coupling to all the possible channels, it cannot be evaluated in practice. For all these reasons, the interactions entering $H_{\rm eff}$ are usually determined phenomenologically, and represented by simple (commonly local) forms.

Once the model space and the effective interactions have been defined, the model wavefunction is expanded in the set of internal states explicitly included (that is, those of the P-space),

$$\Psi^{(+)}_{\rm model} = \sum_{\alpha} \Phi_{\alpha}(\xi_{\alpha}) \chi^{(+)}_{\alpha}(\mathbf{R}_{\alpha}) \tag{1.30}$$

where $\chi^{(+)}_{\alpha}(\mathbf{R}_{\alpha})$ obey the usual outgoing boundary conditions [c.f. Eq. (1.6)].

Chapter 2

Single-channel scattering: the optical model

Direct reaction theories try to reduce the complicated many-body scattering problem to a tractable problem of the form

$$(E - H_{\text{eff}})\Psi_{\text{model}} = 0 \tag{2.1}$$

where H_{eff} is an effective Hamiltonian defined in the model space, that is, the set of channels of interest (in the Feshback language, the P space). The Ψ_{model} will be in general an expansion in the states of the P space.

The crudest approximation to the P space is to reduce the physical space to just the ground state of the projectile and target. This gives rise to the optical model formalism. In this case, the model wavefunction (1.30) is approximated by a single term,[1]

$$\Psi^{(+)}_{\text{model}}(\xi, \mathbf{R}) = \Phi_0(\xi)\chi^{(+)}_0(\mathbf{R}) \tag{2.2}$$

and the effective Hamiltonian is expressed as

$$H_{\text{eff}} = H_\alpha + U_\alpha \tag{2.3}$$

The model wavefunction is a solution of

$$[T_\alpha + H_\alpha + U_\alpha(\mathbf{R}) - E]\Psi^{(+)}_{\text{model}} = 0 \tag{2.4}$$

Using the fact that, by construction, $H_\alpha\Phi_0(\xi) = \varepsilon_0\Phi_0(\xi)$, we get

$$[T_\alpha + U_\alpha(\mathbf{R}) - E_0]\chi^{(+)}_0(\mathbf{R}) = 0 \tag{2.5}$$

where $E_0 = E - \varepsilon_0$, i.e., the kinetic energy associated with the relative motion between the projectile and target.

[1] The subscript α is omitted here when implicitly understood.

If the effective Hamiltonian, $H_{\rm eff}$, is to represent the complicated Feshbach operator, describing not only the interaction in the P space, but also the couplings between the P and Q spaces (all non-elastic channels in this case), then the effective interaction $U_\alpha(\mathbf{R})$ will be complex, non-local and energy-dependent. The imaginary part accounts for the flux leaving the elastic channel (P space) to the channels not explicitly included (the Q space). The energy dependence is usually taken into account phenomenologically, by parametrizing U with some suitable form and adjusting the parameters to the experimental data over some energy region. Finally, non-locality is rarely taken into account. The effective interaction U_α is referred to as **optical potential**.

2.1 Partial wave expansion

As an additional simplification, we consider the case in which the spins of the colliding particles are ignored and the optical potential is assumed to be a function only of the projectile-target separation, $R = |\mathbf{R}|$. In this case, the wave function can expanded in spherical harmonics,

$$\chi_0^{(+)}(\mathbf{K},\mathbf{R}) = \sum_{\ell m} C_{\ell,m} \frac{\chi_\ell(K,R)}{R} Y_{\ell m}(\hat{R}) \tag{2.6}$$

where the radial functions are a solution of

$$\left[-\frac{\hbar^2}{2\mu}\frac{d^2}{dR^2} + \frac{\hbar^2}{2\mu}\frac{\ell(\ell+1)}{R^2} + U(R) - E_0\right]\chi_\ell(K,R) = 0. \tag{2.7}$$

The coefficients $C_{\ell,m}$ are determined imposing that, in the case of zero potential, the solution must be a plane wave, that is

$$U_\alpha = 0 \quad \Rightarrow \quad \chi_0^{(+)}(\mathbf{K},\mathbf{R}) = e^{i\mathbf{K}\cdot\mathbf{R}} \tag{2.8}$$

whose expansion in terms of spherical harmonics is given by

$$e^{i\mathbf{K}\cdot\mathbf{R}} = \frac{4\pi}{KR}\sum_{\ell,m} i^\ell F_\ell(KR) Y_{\ell m}(\hat{R}) Y^*_{\ell m}(\hat{K}) \tag{2.9}$$

$$= \frac{1}{KR}\sum_{\ell} i^\ell (2\ell+1) F_\ell(KR) P_\ell(\cos\theta) \tag{2.10}$$

where $F_\ell(KR) = (KR) j_\ell(K,R)$ with $j_\ell(K,R)$ a spherical Bessel function. Comparing this expression with (2.6), it is convenient to use the coefficients $C_{\ell,m}$ such that in the limit $U \to 0$, the expansion (2.6) reduces to (2.9),

$$\chi_0^{(+)}(\mathbf{K},\mathbf{R}) = \frac{1}{KR}\sum_{\ell} i^\ell (2\ell+1)\chi_\ell(K,R) P_\ell(\cos\theta) \tag{2.11}$$

In the case in which the potential is non-zero, we can still say that $\chi_0^{(+)}(\mathbf{K},\mathbf{R})$ must verify the following equation at large distances,

$$\left[-\frac{\hbar^2}{2\mu}\frac{d^2}{dR^2} + \frac{\hbar^2}{2\mu}\frac{\ell(\ell+1)}{R^2} - E_0\right]\chi_\ell(K,R) = 0 \quad \text{(for large R)} \tag{2.12}$$

and the most general solution will be combination of two independent solutions for this equation. One of them can be taken as the regular solution $F_\ell(KR)$. The other can be the irregular solution,

$$G_\ell(KR) = -(KR)n_\ell(KR) \tag{2.13}$$

or any combination of G and F, that is,

$$\chi_\ell(K,R) \xrightarrow{R\gg} AF_\ell(KR) + BG_\ell(KR) \tag{2.14}$$

The combination appropriate for our purposes is suggested by the known asymptotic behavior of our physical scattering wavefunction, i.e.

$$\chi_0^{(+)}(\mathbf{K},\mathbf{R}) \xrightarrow{R\gg} e^{i\mathbf{K}\cdot\mathbf{R}} + f(\theta)\frac{e^{iKR}}{R} \tag{2.15}$$

The exponential part of the outgoing wave, e^{iKR}, turns out to be just a suitable combination of the F and G functions, because

$$G_\ell(\rho) + iF_\ell(\rho) \equiv H_\ell^{(+)}(\rho) \to e^{i(\rho-\ell\pi/2)} \tag{2.16}$$

So, returning to the partial wave expansion, the appropriate boundary condition consistent with the behavior (2.15) is given by

$$\boxed{\chi_\ell(K,R) \to F_\ell(KR) + T_\ell H_\ell^{(+)}(KR)} \tag{2.17}$$

where the (yet undetermined) coefficient T_ℓ is known as transmission coefficient. It is usual to write T_ℓ in terms of the so-called *phase-shifts*,

$$\boxed{T_\ell = e^{i\delta_\ell}\sin(\delta_\ell)} \tag{2.18}$$

or, in terms of the **reflection coefficient**, S_ℓ, or **S-matrix**,[2]

$$\boxed{S_\ell = 1 + 2iT_\ell = e^{2i\delta_\ell}} \tag{2.19}$$

The condition (2.17) can be also written as,

$$\boxed{\chi_\ell(K,R) \to \frac{i}{2}\left[H_\ell^{(-)}(KR) - S_\ell H_\ell^{(+)}(KR)\right]} \tag{2.20}$$

where

$$H_\ell^{(-)}(\rho) = G_\ell(\rho) - iF_\ell(\rho) \to e^{-i(\rho-\ell\pi/2)} \tag{2.21}$$

The S-matrix S_ℓ is therefore the coefficient of the outgoing wave ($H^{(+)}$) for the partial wave ℓ. It reflects the effect of the potential on this particular wave in the sense that,

[2]When these expressions are generalized to the multiple channel case, the quantity S_ℓ becomes a matrix and is referred to as *scattering or collision matrix* (the name is also used in single-channel case, but the terminology is less obvious).

- If no potential is present, there is no outgoing wave. Then, $T_\ell = 0$ or, equivalently, $S_\ell = 1$ and $\delta_\ell = 0$.

- As a consequence of the previous item, for large values of ℓ the centrifugal barrier keeps the projectile well apart from the target, and thus the effect of the (short-ranged) potential U_α will be negligible. Consequently, for $\ell \to \infty \Rightarrow S_\ell \to 1$.

- If the scattered potential is real, the overall outgoing flux for a given partial wave must be conserved, and hence $|S_\ell| = 1$.

- On the other hand, for a complex potential (with negative imaginary part), we have $|S_\ell| < 1$, thus reflecting that part of the incident flux has left the elastic channel in favor of other channels.

2.2 Scattering amplitude

To get the scattering amplitude, we substitute the asymptotic radial function $\chi_\ell(K,R)$ from (2.20) into the full expansion (2.11):

$$\begin{aligned}\chi_0^{(+)}(\mathbf{K},\mathbf{R}) &\to \frac{1}{KR}\sum_\ell i^\ell(2\ell+1)\left\{F_\ell(KR)+T_\ell H_\ell^{(+)}(KR)\right\}P_\ell(\cos\theta)\\ &= \frac{1}{KR}\sum_\ell i^\ell(2\ell+1)F_\ell(KR)P_\ell(\cos\theta)+\frac{1}{K}\sum_\ell i^\ell(2\ell+1)T_\ell\frac{e^{i(KR-\ell\pi/2)}}{R}P_\ell(\cos\theta)\\ &= e^{i\mathbf{K}\cdot\mathbf{R}}+\frac{1}{K}\sum_\ell(2\ell+1)e^{i\delta_\ell}\sin\delta_\ell P_\ell(\cos\theta)\frac{e^{iKR}}{R}\end{aligned} \tag{2.22}$$

The elastic scattering amplitude is the coefficient of e^{iKR}/R in the last line,i.e.,

$$\begin{aligned}f(\theta) &= \frac{1}{K}\sum_\ell(2\ell+1)e^{i\delta_\ell}\sin\delta_\ell P_\ell(\cos\theta)\\ &= \frac{1}{2iK}\sum_\ell(2\ell+1)(S_\ell-1)P_\ell(\cos\theta).\end{aligned} \tag{2.23}$$

The differential elastic cross section will be given by

$$\frac{d\sigma}{d\Omega} = |f(\theta)|^2. \tag{2.24}$$

In principle, the sum in (2.23) runs from $\ell = 0$ to infinity. However, remember that, for large values of ℓ, the S-matrix tends to 1 so, in practice, the sum can be safely truncated at a maximum value $\ell_{\max}$, determined by some convergence criterion of the cross section.

2.3 Coulomb case

The Coulomb case deserves a special consideration because the expressions derived in the previous section are strictly applicable to the case of short-range potentials, for which the asymptotic form (2.15) is appropriate. For a pure Coulomb case, we can perform a partial wave expansion of the scattering wavefunction $\chi_C(\mathbf{K},\mathbf{R})$ of the form

$$\chi_C(\mathbf{K},\mathbf{R}) = \frac{1}{KR}\sum_\ell (2\ell+1) i^\ell \chi_\ell^C(KR) P_\ell(\cos(\theta)) \tag{2.25}$$

with the radial functions $\chi_\ell^C(KR)$ obeying the equation

$$\left[\frac{d^2}{dR^2} + K^2 - \frac{2\eta K}{R} + \frac{\ell(\ell+1)}{R^2}\right]\chi_\ell^C(KR) = 0 \tag{2.26}$$

where

$$\eta = \frac{Z_p Z_t e^2}{\hbar v} = \frac{Z_p Z_t e^2 \mu}{\hbar^2 K} \tag{2.27}$$

the so-called Coulomb or **Sommerfeld parameter**.

The solution of (2.26) must be regular at the origin. Asymptotically, it behaves as

$$\chi_\ell^C(KR) \xrightarrow{R\gg} e^{i\sigma_\ell} F_\ell(\eta, KR) \tag{2.28}$$

where $F_\ell(\eta, KR)$ is the regular Coulomb function and σ_ℓ is the Coulomb phase-shift for a partial wave ℓ,

$$\sigma_\ell = \arg\Gamma(\ell+1+i\eta) \tag{2.29}$$

The Coulomb function behaves asymptotically as

$$F_\ell(\eta,\rho) \to \sin(\rho - \eta\ln(2\rho) - \ell\pi/2 + \sigma_\ell) \tag{2.30}$$

which in the case $\eta = 0$ ($\sigma_\ell = 0$) reduces to the regular $F_\ell(KR)$ function introduced in the case of short-range potentials

$$F_\ell(\eta = 0, \rho) = F_\ell(\rho) = \rho j_\ell(\rho) \tag{2.31}$$

Analogously, an irregular solution of (2.26) can be found, which reduces to $G_\ell(\rho)$ in the no Coulomb case

$$G_\ell(\eta,\rho) \to \cos(\rho - \eta\ln(2\rho) - \ell\pi/2 + \sigma_\ell) \xrightarrow{\eta=0} G_\ell(\rho) = -\rho n_\ell(\rho) \tag{2.32}$$

as well as the ingoing and outgoing functions,

$$H^{(+)}(\eta,\rho) = G_\ell(\eta,\rho) + iF_\ell(\eta,\rho) \tag{2.33}$$

$$H^{(-)}(\eta,\rho) = G_\ell(\eta,\rho) - iF_\ell(\eta,\rho) \tag{2.34}$$

For the pure Coulomb case, the scattering amplitude will be given by

$$f_C(\theta) = \frac{1}{2K}\sum_\ell (2\ell+1)(e^{2i\sigma_\ell}-1)P_\ell(\cos\theta) \tag{2.35}$$

This integral is not convergent (cannot be truncated at a finite ℓ) but the full result is known analytically and is given by

$$f_C(\theta) = -\frac{\eta}{2K\sin^2(\frac{1}{2}\theta)} e^{-i\eta\ln(\sin^2(\frac{1}{2}\theta)+2i\sigma_0)} \tag{2.36}$$

The differential cross section yields the well-known Rutherford formula

$$\frac{d\sigma_R}{d\Omega} = |f_C(\theta)|^2 = \frac{\eta^2}{4K^2\sin^4(\frac{1}{2}\theta)} = \left(\frac{Z_pZ_te^2}{4E}\right)^2 \frac{1}{\sin^4(\frac{1}{2}\theta)} \tag{2.37}$$

2.4 Coulomb plus nuclear case

If both Coulomb and nuclear potentials are present, the scattering function $\chi_0^{(+)}(\mathbf{K},\mathbf{R})$ will never reach the asymptotic form of a plane wave plus outgoing waves, due to the presence of the $1/R$ term in Schrödinger equation. Nevertheless, it can be written as

$$\chi_0^{(+)}(\mathbf{K},\mathbf{R}) \to \chi_C^{(+)}(\mathbf{K},\mathbf{R}) + \text{outgoing spherical waves} \tag{2.38}$$

where the *outgoing waves* part are now proportional to the functions $H_\ell^{(+)}(\eta, KR)$. Of course, when only the Coulomb potential is present, this term vanishes, and the scattering wavefunction reduces to $\chi_C^{(+)}(\mathbf{K},\mathbf{R})$.

If we write, as usual, the $\chi_0^{(+)}(\mathbf{K},\mathbf{R})$ as a partial wave expansion, the corresponding radial coefficients $\chi_\ell(K,R)$ verify the asymptotic condition

$$\chi_\ell(K,R) \to e^{i\sigma_\ell}\left[F_\ell(\eta,KR) + T_\ell H_\ell^{(+)}(\eta,KR)\right] \tag{2.39}$$

$$= e^{i\sigma_\ell}\frac{i}{2}\left[H_\ell^{(-)}(\eta,KR) - S_\ell H_\ell^{(+)}(\eta,KR)\right] \tag{2.40}$$

which is very similar to (2.17) and (2.20), expect for additional Coulomb phase $e^{i\sigma_\ell}$ and replacement of the functions $F(KR)$, $H^{(+)}$, etc by their Coulomb generalizations.

The scattering amplitude results

$$f(\theta) = f_C(\theta) + \frac{1}{2iK}\sum_\ell (2\ell+1)e^{2i\sigma_\ell}(S_\ell-1)P_\ell(\cos\theta) \tag{2.41}$$

where the first term corresponds to the pure-Coulomb amplitude, and arises from the outgoing waves in the first term of (2.38).

Numerical calculation of the scattering wavefunction and phase-shifts

In practice, the calculations of the scattering wave function and the corresponding reflection coefficients (or phase-shifts) are usually computed as follows:

1. Integrate the radial differential equation from the origin outwards, with the initial value $\chi_\ell(K,0)=0$ and some finite (arbitrary) slope.
2. At a sufficiently large distance, $R_{\max}$, beyond which the nuclear potentials have become negligible, the numerically obtained solution is matched to the asymptotic form
$$N\chi_\ell(K,R_{\max}) \to F_\ell(\eta,KR_{\max}) + T_\ell H_\ell^{(+)}(\eta,KR_{\max}) \tag{2.42}$$
3. This equation contains two unknowns, T_ℓ and the normalization N. Thus, it is supplemented with the condition of continuity of the derivative
$$N\chi'_\ell(K,R_{\max}) \to F'_\ell(\eta,KR_{\max}) + T_\ell (H_\ell^{(+)}(\eta,KR_{\max}))' \tag{2.43}$$
4. The procedure is repeated for each ℓ, from $\ell=0$ to $\ell_{\max}$, such that $S_{\ell_{\max}}\approx 1$.

2.5 Parametrization of the phenomenological optical potential

The effective optical optical potential is usually taken as the sum of Coulomb and nuclear central potentials $U(R)=U_{nuc}(R)+U_{coul}(R)$, with the Coulomb part taken as the potential corresponding to a uniform distribution of charge of radius R_c:

$$U_c(R) = \begin{cases} \frac{Z_1Z_2e^2}{2R_c}\left(3-\frac{R^2}{R_c^2}\right) & \text{if } R\le R_c \\ \frac{Z_1Z_2e^2}{R} & \text{if } R\ge R_c \end{cases} \tag{2.44}$$

As for the nuclear part, it contains in general real and imaginary parts. The most standard parametrization is that of Woods-Saxon

$$U_{\rm nuc}(R) = V(R)+iW(R) = -\frac{V_0}{1+\exp\left(\frac{R-R_0}{a_0}\right)} - i\,\frac{W_0}{1+\exp\left(\frac{R-R_i}{a_i}\right)} \tag{2.45}$$

The parameters V_0, R_0 and a_0 are the depth, radius and diffuseness (likewise for the imaginary part). They are usually determined from the analysis of elastic scattering data.

If the spin-of the projectile (or target) is considered, the potential will contain also spin-dependent term. The most common one is the spin-orbit term, which is usually

parametrized as

$$U_{so}(R) = (V_{so} + iW_{so}) \left(\frac{\hbar}{m_\pi c}\right)^2 \frac{1}{R} \frac{df(R, R_{so}, a_{so})}{dR} (2\ell \cdot \mathbf{s}) \tag{2.46}$$

where the radial function $f(R, R_{so}, a_{so})$ is again a Woods-Saxon form, and $(\hbar/m_\pi c)^2 = 2$ fm^2, is just introduced in order U_{so} have dimensions of energy.

Chapter 3

Inelastic scattering

Nuclei are not inert or *frozen* objects; they do have an internal structure of protons and neutrons that can be modified (excited), for example, in collisions with other nuclei. In fact, a important and common process that may occur in a collision between two nuclei is the excitation of one (or both) of the nuclei.

Inelastic scattering is an example of *direct reaction* (see Chapter 1) and, as such, the colliding nuclei preserve their collision after the collision.

The energy required to excite a nucleus is *taken* from the kinetic energy associated with projectile-target relative motion. This means that, if one of the colliding nuclei is excited, the final kinetic energy of the system is reduced by an amount equal to the excitation energy of the excited state populated in the reaction. So, by measuring the kinetic energy of the outgoing fragments, one can infer the excitation energy of the projectile and target. This has been indeed a common technique to identify such excited states.

The information provided by the analysis of inelastic reactions is not restricted to the level spectrum of nuclei. By comparing the energy and angular distribution of the ejectile with an appropriate reaction theory, we can infer also useful structure information, such as the spin and parity of the populated states, the electric transition probabilities connecting these states, the deviation from the spherical shape in deformed systems, etc

3.1 Collective versus single-particle excitations

Nuclei, like atoms, tend to be in their state of minimal energy (the so-called ground state) which corresponds to a certain arrangement of protons and neutrons inside the nucleus. The excitation of the nucleus corresponds microscopically to a rearrangement of protons and neutrons. This is a many-body quantum-mechanical problem, which can be very difficult to treat in a general situation. However, in many cases, it is possible to rely on a simpler picture, which emphasize some particular degree of freedom of the system. This is the case of the single-particle excitations observed in even-odd nuclei, or that of collective excitations due to the rotation or vibration of the nucleus.

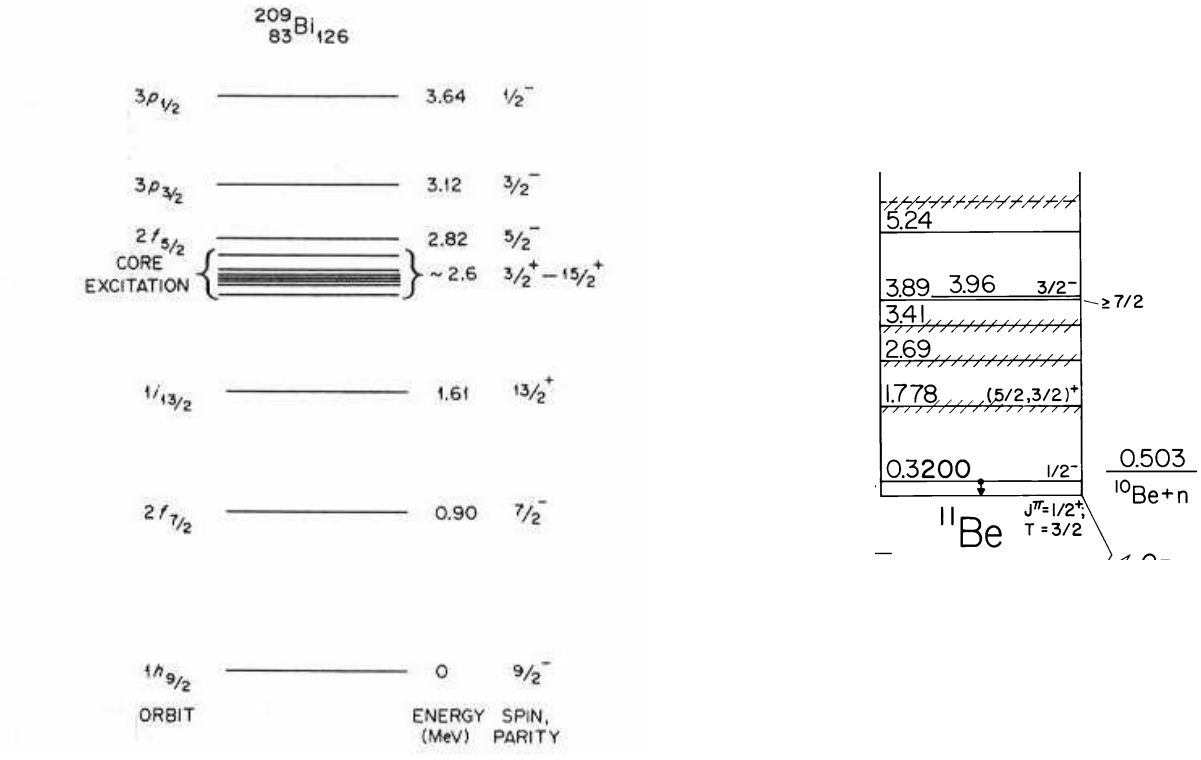

Figure 3.1: Energy levels of ^{209}Bi and ^{11}Be, interpreted as single-particle excitations.

- **Single-particle excitations:** If we have a nucleus with one "valence" nucleon outside a closed shell, there will be low excited states which corresponds to promoting this odd nucleon into higher shell-model orbits without disturbing the inner closed shells. Two examples are shown in Fig. 3.1. In the ^{209}Bi case, the first 82 protons constitute a relatively inert core and the remaining proton moves in the average potential created by this core.

  The second example shown in Fig. 3.1 is ^{11}Be, which is an example of "exotic" nucleus. The excess of neutrons ($N = 7$ versus $Z = 4$) makes this system very unstable, decaying into ^{11}B by β^- emission ($T_{1/2} = 13.76$ s). The ground state ($1/2^+$) can be interpreted in a single-particle picture as a neutron moving around a ^{10}Be core in a $2s_{1/2}$ orbital. Very close to the ground state, at $E_x = 320$ keV, there is a $1/2^-$ excited state, which can be obtained promoting the last neutron the $1p_{1/2}$ orbital[1].

- **Collective excitations:** Some excited states are not easily interpreted in terms of single-particle excitations, even considering more than one active nucleon. However, in many cases they can be interpreted as collective excitations of the nucleus as a

[1]Note that this is not the expected sequence of stable nuclei, for which one would expect the $1p_{1/2}$ orbital to be below the $2s_{1/2}$ orbital. This parity inversion is a consequence of the proton/neutron asymmetry and is subject nowadays of many studies.

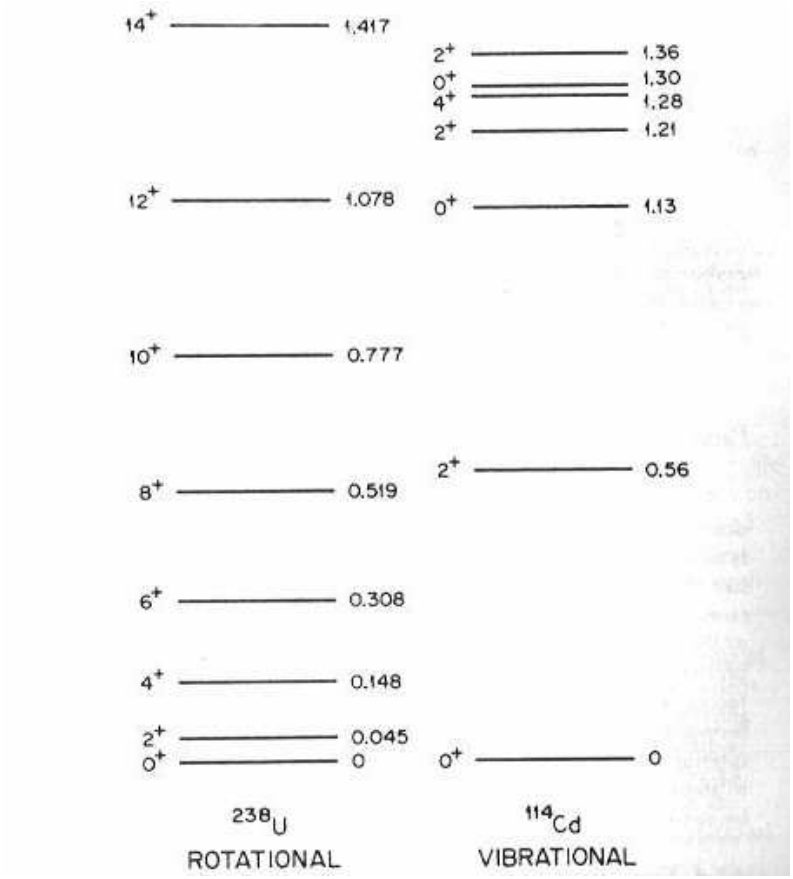

Figure 3.2: Energy levels of a typical rotational (left) and a typical vibrational (right) nucleus.

whole. This is the case of nuclei with a permanent deformation in which excited states correspond to the rotational motion of the nucleus, slowly rotating as a whole. In the pure rotational model, the energy spectrum is of the form

$$E(I) = \frac{\hbar^2}{2\mathcal{I}} \left[I(I+1) - K(K+1) \right], \tag{3.1}$$

where I is spin of the level with excitation energy $E(I)$, K is the projection of the angular momentum along the symmetry axis of the deformed system and $\mathcal{I}$ is the moment of inertia of the nucleus. For even-even nuclei, the ground state has $I = 0$ and hence the rotational band built on top of the ground state has $K = 0$ too. Physically, this means that the rotation occurs about an axis perpendicular to the nuclear symmetry axis. It can be shown that in this case only even values of I appear. An example of rotational spectrum for an even-even nucleus is shown in the left-hand-side of Fig. 3.2.

Another example of collective excitations are the *vibrations* experienced by an spherical nucleus. These can be visualized as harmonic oscillations of the surface about

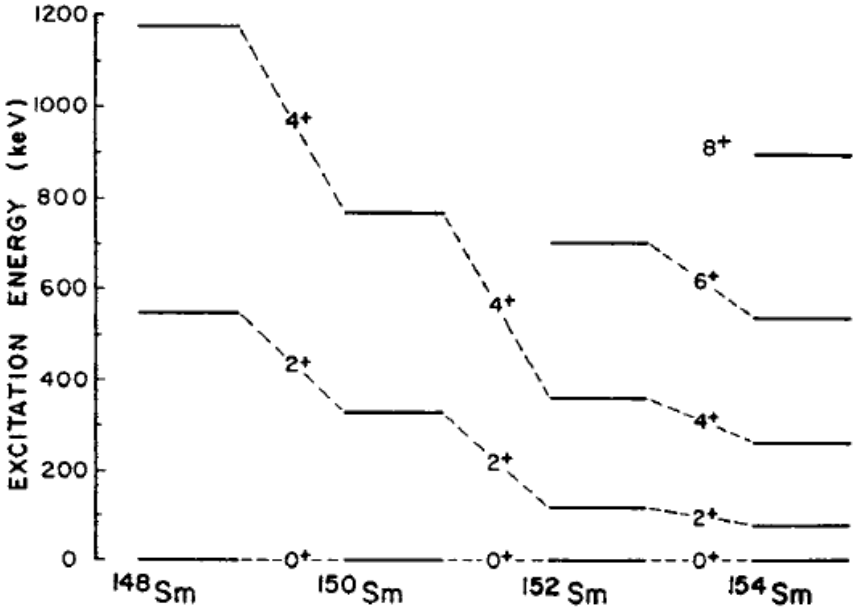

Figure 3.3: Energy levels of samarium isotopes showing the evolution from a typical vibrational spectrum in ^{148}Sm to a rotational spectrum fully developed in ^{152}Sm and ^{154}Sm. Quoted from Ref. [11], p. 229.

the spherical shape. In an even-even nucleus, the corresponding energy spectrum for a multipolarity λ consists of evenly spaced levels with

$$E_n = n\hbar\omega_\lambda$$

where $n = 0, 1, \ldots$ is the number of phonons, each carrying an energy of $\hbar\omega_\lambda$ and angular momentum $\lambda\hbar$. For example, for quadrupole phonons (λ=2), $n = 0$ corresponds to the state with no phonons, and has $I = 0$. This is the ground state of the system. For $n = 1$ phonon, we have a (excited) state with $I = 2$ angular momentum and energy $\hbar\omega_\lambda$. With two quadrupole phonons ($n = 2$), we get an excited state with energy $2\hbar\omega_\lambda$. Since each phonon carries an angular momentum of $2\hbar$, they can couple to angular momenta I=0, 2 and 4, so we actually have 3 degenerated levels.

An example of vibrational spectrum is shown in the right-hand-side of Fig. 3.2, corresponding to the ^{114}Cd nucleus. The 0^+, 2^+ and 4^+ triplet of states around $E_x \approx$ 1 MeV corresponds to the excitation of two quadrupole phonons. The additional 0^+ and 2^+ states observed nearby are due to a different kind of excitation.

It is worth noting that the vibrational or rotational character can change from an isotope to another within the same isotopic chain. An example is shown in Fig. 3.3, for the first levels of the samarium isotopes, exhibiting the characteristic level spacing of vibrator and rotor at the extremes.

There are other kinds of collective excitations (monopole, giant resonances, etc) but they will not be considered here.

3.2 Energy balance considerations

We start by recalling the concept of Q-value. Consider the binary direct reaction $a+A \to b+B$, where a projectile a collides with a target A giving rise to an ejectile b and a residual nucleus B. Due to energy conservation in the CM frame,

$$E^i_{\rm cm} + M_a c^2 + M_A c^2 = E^f_{\rm cm} + M_b c^2 + M_B c^2, \tag{3.2}$$

where $E^i_{\rm cm}$ ($E^f_{\rm cm}$) is the total kinetic energy in the initial (final) channels. It is customary to introduce the Q-value, defined as

$$Q = M_a c^2 + M_A c^2 - M_b c^2 - M_B c^2. \tag{3.3}$$

In terms of Q, the energy balance can be expressed as

$$E^f_{\rm cm} = E^i_{\rm cm} + Q. \tag{3.4}$$

For $Q > 0$ we have $E^f_{\rm cm} > E^i_{\rm cm}$ and the reaction is said to be **exothermic**. Conversely, for $Q < 0$ we have $E^f_{\rm cm} < E^i_{\rm cm}$ and the reaction is said to be **endothermic**.

For an inelastic process, the nuclei are the same in the initial and final channels. Let us assume, for definiteness, that the projectile is excited to an excited state E_x. Then, the energy balance becomes in this case

$$E^i_{\rm cm} + M_a c^2 + M_A c^2 = E^f_{\rm cm} + M^*_a c^2 + M_A c^2, \tag{3.5}$$

where $M^*_a = M_a + E_x$.

In this case, the Q-value is simply given by

$$Q = M_a c^2 + M_A c^2 - M^*_a c^2 - M^2_A = -E_x,$$

that is, $Q = -E_x < 0$. Consequently, an inelastic reaction is always endothermic. This is not unexpected, since part of the kinetic energy is used to excite one of the nuclei.

From these considerations, we see that the excitation energy of the states populated in a inelastic process can be inferred by just measuring the kinetic energy of the outgoing fragments. In fact, this is a powerful technique to obtain the energy spectrum of a nucleus.

Example: the p+^{7}Li reaction

As an example, let us consider the scattering of a proton beam by a ^{7}Li target. In Fig. 3.4, we see the experimental excitation energy spectrum inferred from the energy of the outgoing protons detected at an scattering angle of 25°. We have superimposed the known energy spectrum of ^{7}Li to emphasize the correspondence between the observed

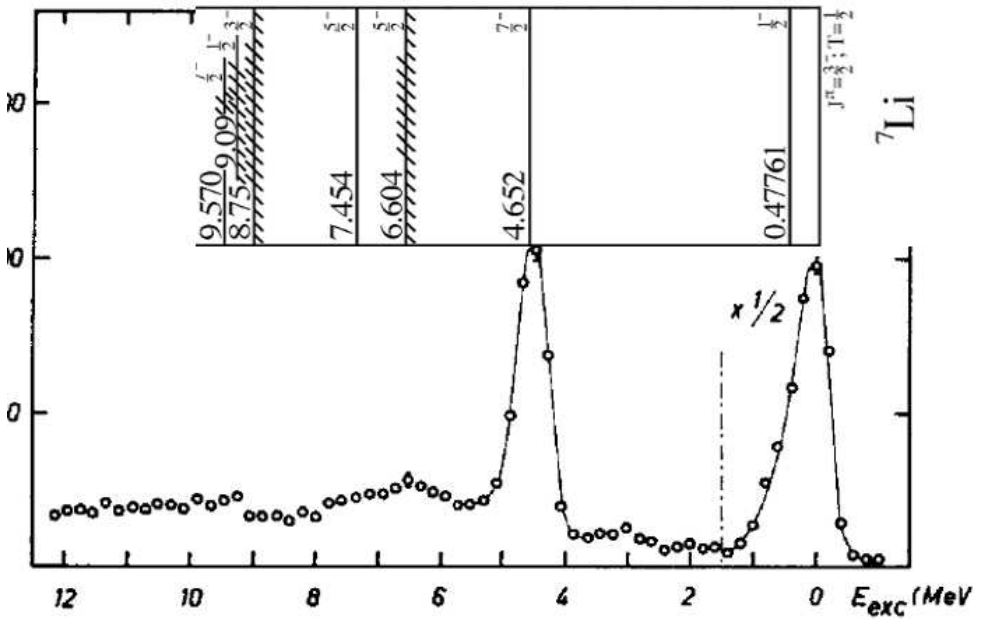

Figure 3.4: Energy spectrum of detected outgoing protons scattered from a ^{7}Li target (quoted from Ref. [14]).

peaks and these states. The peak at $E_x = 0$ (corresponding to $Q = 0$) corresponds to the ground state of ^{7}Li. Thus, it is just elastic scattering. At $E_x = 0.48$ MeV, we should see a second peak corresponding to the first excited state of ^{7}Li. However, due to the energy resolution, this peak is not resolved in these data from the elastic peak. At $E_x = 4.6$ MeV there is a prominent peak corresponding to a $7/2^-$ state in ^{7}Li. This state is above the ^{4}He+t threshold and does actually correspond to a continuum resonance. This threshold corresponds to the energy necessary to dissociate the ^{7}Li nucleus into ^{4}He+t. Therefore, for excitation energies above this value, we have a continuous of accessible energies, rather than a discrete spectrum, and any value of E_x is possible. This explains the *background* observed at these excitation energies.

Note that the information provided by these data is not enough to determine other properties of the energy spectrum, such as as the spin/parity assignment or their collective/single-particle character. To do that, one needs to compare the data with a suitable reaction calculation, as we will see in the next section.

3.3 Formal treatment of inelastic reactions

3.3.1 The coupled-channels (CC) method

Remember from Chapter 1 (Sec. 1.4) that any practical solution of the scattering problem starts with a reduction of the full physical space into P and Q spaces, the former

corresponding to the channels that are to be explicitly included. In an inelastic process, this P space will consist of the elastic channel, plus some excited states of the projectile and/or target, those more strongly coupled in the process or, at least, those that will be compared with the experimental data.

Let us consider the scattering of a projectile a by a target A, and let us assume for simplicity that only the projectile can be excited during the process, the target being just an inert spectator. We denote this mass partition by the index α, i.e., $\alpha \equiv a + A$. Our model Hamiltonian will describe a set of states of the projectile, and the coupling between during the collision. This model Hamiltonian will be expressed as:

$$H = -\frac{\hbar^2}{2\mu_{aA}}\nabla^2_{\mathbf{R}} + H_a(\xi) + V_\alpha(\xi, \mathbf{R}) \tag{3.6}$$

where $V_\alpha(\xi, \mathbf{R})$ is the projectile-target interaction and $H_a(\xi)$ is the internal Hamiltonian of the projectile[2]. The symbol ξ denotes the set of internal coordinates of a. For example, in deuteron scattering, ξ may refer to the relative coordinate between the proton and the neutron[3]. $\mathbf{R}$ is the relative coordinate between a and A.

Let us denote by $\{\phi_n(\xi)\}$ the internal states of the projectile. These will be the eigenstates of the Hamiltonian $H_a(\xi)$:

$$H_a\phi_n = \varepsilon_n\phi_n. \tag{3.7}$$

The key idea of the CC method is to expand of the total wavefunction of the system the set of internal states $\{\phi_n(\xi)\}$,

$$\Psi^{(+)}(\mathbf{R}, \xi) = \phi_0(\xi)\chi_0(\mathbf{R}) + \sum_{n>0}^{N} \phi_n(\xi)\chi_n(\mathbf{R}) \tag{3.8}$$

with $\phi_0(\xi)$ representing the ground-state wavefunction and N the number of states included.

The unknown coefficients $\chi_n(\mathbf{R})$ describe the relative motion between the projectile and target in the corresponding internal states. They have a definite physical meaning. They tell us the relative "probability", as a function of $\mathbf{R}$, for the projectile (or target) being in state n. The different possibilities for n are frequently referred to as "channels". The total wavefunction $\Psi(\mathbf{R}, \xi)$ verifies the Schrödinger equation:

$$[E - H]\Psi^{(+)}(\mathbf{R}, \xi) = 0.$$

We now proceed as follows:

- Use the expansion (3.8) and the Hamiltonian (3.6) in this equation.

[2]If both the projectile and target can be excited, we can generalize the equation above by including also the internal Hamiltonian of the target, so $H_a(\xi)$ should be replaced by $H_\alpha = H_a(\xi) + H_A(\xi')$.

[3]The intrinsic spins of the proton and neutron, could be also part of these set of internal coordinates.

- Multiply on the left by each of the basis functions $\phi_n^*(\xi)$, and integrate over the internal coordinates ξ.
- For each n, we get a differential equation of the form:

$$\left[E - \varepsilon_n - \hat{T}_{\mathbf{R}} - V_{n,n}(\mathbf{R})\right] \chi_n(\mathbf{R}) = \sum_{n' \neq n} V_{n,n'}(\mathbf{R}) \chi_{n'}(\mathbf{R}) \tag{3.9}$$

  where $\hat{T}_{\mathbf{R}}$ is the kinetic energy operator and $V_{n,n'}$ are the so called *coupling potentials*, defined by:

$$V_{n,n'}(\mathbf{R}) = \int d\xi \phi_n^*(\xi) V(\xi, \mathbf{R}) \phi_{n'}(\xi) \tag{3.10}$$

  Thus, for example, $V_{0,m}$ is the potential responsible for the excitation from the ground state ($n = 0$) to a given final state m. We have still not defined the form of the effective potential $V(\xi, \mathbf{R})$ and the internal states ϕ_n, that is, the model Hamiltonian. These potentials are constructed within a certain model, as we will see later.

Note that in the equation for a given value of n, we have the unknown $\chi_n(\mathbf{R})$, but also those $\chi_{n'}(\mathbf{R})$ with $n' \neq n$. Consequently, Eq. (3.9) represents a set of coupled differential equations for the set of functions $\{\chi_n(\mathbf{R})\}$.

Boundary conditions

Similarly to the OM case, the CC equations have to be solved with the appropriate boundary conditions. These boundary conditions correspond to the physical situation in which the projectile is initially in the ground-state (ϕ_0) and the projectile-target relative motion is represented by a plane wave with momentum $\mathbf{K}_0$[4]. The situation is schematically represented in Fig. 3.5. Classically, the direction of the momentum $\mathbf{K}_0$ corresponds to the direction of motion of the projectile. As a result of the collision with the target, a serial of outgoing spherical waves is created. That is, the general structure of the wave function of the system is of the form

$$\Psi^{(+)}_{\mathbf{K}_0}(\mathbf{R}, \xi) = e^{i\mathbf{K}_0 \cdot \mathbf{R}} \phi_0(\xi) + (\text{outgoing spherical waves})$$

Unlike the planes waves, the spherical waves scatter in all directions. In addition to the outgoing waves corresponding to elastic scattering, there will be outgoing channels for all the open channels (that is, all the possible final states allowed by energy conservation). So, outside the range of the potentials, the total wave function satisfies:

$$\Psi^{(+)}_{\mathbf{K}_0}(\mathbf{R}, \xi) \xrightarrow{R \gg} \left\{ e^{i\mathbf{K}_0 \cdot \mathbf{R}} + f_{0,0}(\theta) \frac{e^{iK_0 R}}{R} \right\} \phi_0(\xi) + \sum_{n>0} f_{n,0}(\theta) \frac{e^{iK_n R}}{R} \phi_n(\xi), \tag{3.11}$$

[4] A more realistic description would be in terms of wave-packets but the formal treatment is much more complicated. To link both pictures, one can bear in mind that a wave packet can be constructed as a superposition of plane waves.

Comparing with (3.8) we see that the functions $\chi_n(\mathbf{R})$ must verify following boundary conditions:

$$\begin{aligned} \chi_0^{(+)}(\mathbf{K}_0,\mathbf{R}) &\to e^{i\mathbf{K}_0\cdot\mathbf{R}} + f_{0,0}(\theta)\frac{e^{iK_0R}}{R} && n=0 \quad \text{(elastic)} \\ \chi_n^{(+)}(\mathbf{K}_n,\mathbf{R}) &\to f_{n,0}(\theta)\frac{e^{iK_nR}}{R}, && n\neq 0 \quad \text{(non-elastic)} \end{aligned} \tag{3.12}$$

where the superscript "+" indicates that this is the solution which contains *outgoing* spherical waves (one can construct also a solution with ingoing spherical waves that behave as $\exp(-iK_0R)/R$. The coefficient of the outgoing wave $\exp(-iK_0R)/R$, $f_{n,0}(\theta)$, is just the **scattering amplitude**. Once we have determined the scattering amplitude, the cross section is calculated as (c.f. Chapter 1)

$$\boxed{\frac{d\sigma(\theta)}{d\Omega}(0\to n) = \frac{K_n}{K_0}|f_{n,0}(\theta)|^2} \tag{3.13}$$

Note that:

- There are only incoming waves for the χ_0 component (that is, the elastic component) but outgoing waves for all components.

- The scattering angle in the c.m. frame, θ, is determinted by the direction of the momenta $\mathbf{K}_0$ and $\mathbf{K}_n$. Defining the *momentum transfer* as $\mathbf{q} = \mathbf{K}_n - \mathbf{K}_0$, we have (see Fig. 3.5):
$$q^2 = K_0^2 + K_n^2 - 2K_0K_n\cos(\theta) \tag{3.14}$$

- The modulus of the momentum $\mathbf{K}$ is related to the kinetic energy of the system in channel n in the CM frame:
$$E_{\rm cm}^n = \frac{\hbar^2K_n^2}{2\mu}$$

- Due to energy conservation[5],
$$E = \varepsilon_0 + \frac{\hbar^2K_0^2}{2\mu} = \varepsilon_n + \frac{\hbar^2K_n^2}{2\mu}$$

[5]For $\varepsilon_n > E$, the kinetic energy is negative and the corresponding momentum K_n becomes imaginary. Consequently, the asymptotic solutions χ_n of Eq. (3.12) vanish exponentially and then these channels do not contribute to the outgoing flux.

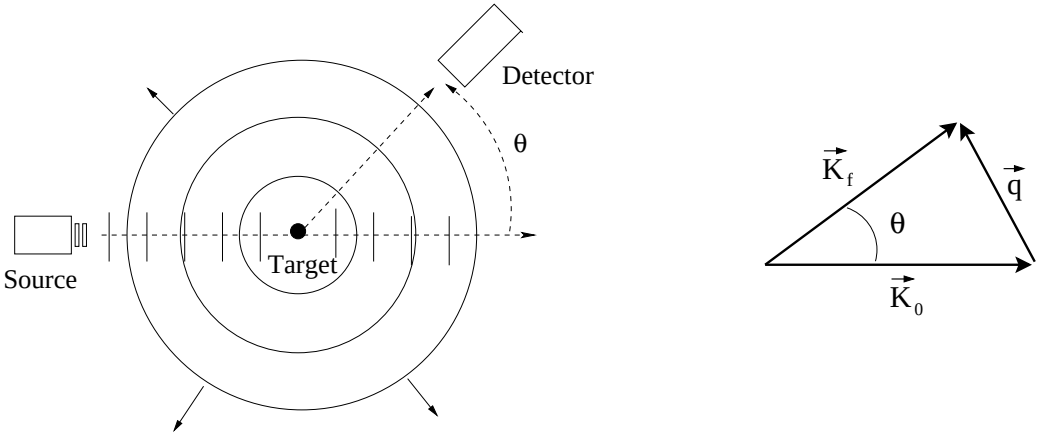

Figure 3.5: Left: incident and scattered waves in a scattering process. Right: incident and final momenta, and momentum transfer

3.3.2 The DWBA method

If the number of states is large, the solution of the coupled equations can be a difficult task. In many situations, however, some of the excited states are very weakly coupled to the ground state and can be treated perturbatively. In this case, the set of equations (3.9) can be solved iteratively, starting from the elastic channel equation, and setting to zero the source term (the RHS of the equation). This allows the calculation of the distorted wave $\chi_0(\mathbf{K}_0, \mathbf{R})$. This solution is then inserted into the equation corresponding to an excited state n, thus providing a first order approximation for $\chi_n(\mathbf{K}_0, \mathbf{R})$. If the process is stopped here, then the method is referred to as *distorted wave Born approximation* (DWBA).

We provide here an alternative derivation of the DWBA method, which leads to a more direct connection with the scattering amplitude. We make use of the *exact* scattering amplitude (1.23) derived in Chapter 1 using the Gell-Mann–Goldberger transformation, and that we reproduce here for completeness:

$$\mathcal{T}_{\beta,\alpha} = \mathcal{T}^{(0)}_{\beta,\alpha}\delta_{\alpha\beta} + \int\int \chi^{(-)*}_{\beta}(\mathbf{K}_\beta, \mathbf{R}_\beta)\Phi^*_\beta(\xi_\beta) W_\beta \Psi^{(+)}_{\mathbf{K}_\alpha} d\xi_\beta d\mathbf{R}_\beta \ , \tag{3.15}$$

where $W_\beta = V_\beta - U_\beta$. Let us particularize to our case, assuming that we are to describe a transition between an initial state i (typically, the g.s.) and a final state f. Since these states belong to the same partition (α) we do not need to specify explicitly the subscript α or β. Then, the expression above becomes

$$\mathcal{T}_{f,i} = \int\int \chi^{(-)*}_{f}(\mathbf{K}_f, \mathbf{R})\phi^*_f(\xi)[V_f - U_f]\Psi^{(+)}_{\mathbf{K}_i} d\xi d\mathbf{R}\,, \tag{3.16}$$

where, within the CC method, $\Psi^{(+)}_{\mathbf{K}_i}$ is given by the expansion (3.8). Recall that, in this

expression $\chi_f^{(-)}(\mathbf{K}_f, \mathbf{R})$ is the time reverse of $\chi_f^{(+)}(\mathbf{K}_f, \mathbf{R})$, which is a solution of

$$[\hat{T}_{\mathbf{R}} + U_f + \varepsilon_f - E]\chi_f^{(+)}(\mathbf{K}_f, \mathbf{R}) = 0 \tag{3.17}$$

for some auxiliary potential $U_f(\mathbf{R})$. Typically, $U_f(\mathbf{R})$ is chosen as a phenomenological potential that describes the elastic scattering in the final channel.

In DWBA, the wavefunction of the system in the initial state is approximated by:

$$\Psi_i^{(+)}(\mathbf{R}, \xi) \simeq \chi_i^{(+)}(\mathbf{K}_i, \mathbf{R})\phi_i(\xi), \tag{3.18}$$

where $\chi_i^{(+)}(\mathbf{K}, \mathbf{R})$ is the distorted wave describing the projectile-motion in the entrance channel,

$$\left[E - \varepsilon_i - \hat{T}_{\mathbf{R}} - U_i(\mathbf{R})\right] \chi_i^{(+)}(\mathbf{K}_i, \mathbf{R}) = 0\,, \tag{3.19}$$

where $U_i(\mathbf{R})$ is the average potential in the initial channel, and is usually taken as the potential that describes the elastic scattering in this channel. With this choice, one hopes to include effectively some of the effects of the neglected channels.

In DWBA, the scattering amplitude corresponding to the inelastic excitation of the projectile from the initial state $\phi_i(\xi)$ and momentum $\mathbf{K}$ to a final state $\phi_f(\xi)$ and momentum $\mathbf{K}_f$ is given by (for details, see for example Ref. [26])

$$\boxed{f_{f,i}^{\mathrm{DWBA}}(\theta) = -\frac{\mu}{2\pi\hbar^2}\int d\mathbf{R}\chi_f^{(-)*}(\mathbf{K}_f, \mathbf{R})W_{if}(\mathbf{R})\chi_i^{(+)}(\mathbf{K}_i, \mathbf{R})} \tag{3.20}$$

where $W_{if}(\mathbf{R})$ is the coupling potential

$$\boxed{W_{if}(\mathbf{R}) \equiv \langle\phi_f|V_f - U_f|\phi_i\rangle = \int d\xi\phi_f^*(\xi)(V_f - U_f)\phi_i(\xi)} \tag{3.21}$$

Actual applications of the DWBA amplitude (3.20) require the specification of the structure model (that will determine the functions $\{\phi_i(\xi)\}$ as well as the projectile-target interaction V_f. We give some examples in the following section.

3.4 Application of the DWBA method to collective excitations

3.4.1 Coulomb excitation

Let us consider the Coulomb potential between a composite projectile of charge $Z_p e$ and a target nucleus of charge $Z_t e$. We ignore the structure of the target but we consider explicitly the internal structure of the projectile (see Fig. 3.6). Consequently, the Coulomb potential is the sum of the interaction with all the protons of the projectile, that is,[6]

$$V(\mathbf{R}, \xi) = \sum_i^{Z_p} \frac{\kappa Z_t e^2}{|\mathbf{R} - \mathbf{r}_i|}, \tag{3.22}$$

[6]In many textbooks and papers, it is customary to use units in which $\kappa = 1$.

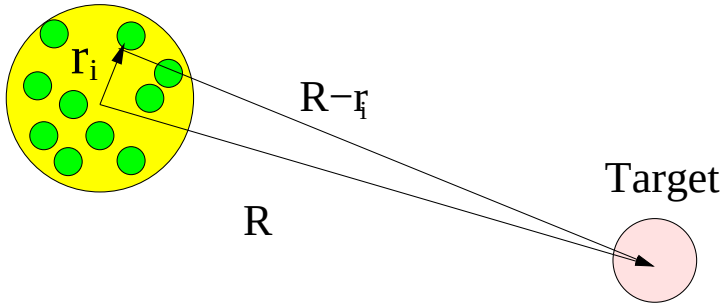

Figure 3.6: Coulomb interaction between a particle and a composite system.

with $\kappa \equiv 1/4\pi\epsilon_0$ and $\xi = \{\mathbf{r}_i\}$. .

We use the following multipole expansion, which is valid for $R > r_i$:

$$\frac{1}{|\mathbf{R} - \mathbf{r}_i|} = \sum_{\lambda\mu} \frac{4\pi}{2\lambda+1} \frac{r_i^\lambda}{R^{\lambda+1}} Y_{\lambda\mu}(\hat{r}_i) Y^*_{\lambda\mu}(\hat{R}) \qquad (R > r_i) \tag{3.23}$$

This allows to express the Coulomb potential in terms of the so-called *multipole electric operator*, defined as:

$$M(E\lambda, \mu) \equiv e \sum_i^{Z_p} r_i^\lambda Y_{\lambda\mu}(\hat{r}_i), \tag{3.24}$$

giving rise to

$$V(\mathbf{R}, \xi) = \sum_{\lambda,\mu} \frac{4\pi}{2\lambda+1} \frac{\kappa Z_t e}{R^{\lambda+1}} M(E\lambda, \mu) Y^*_{\lambda\mu}(\hat{R}), \tag{3.25}$$

where $\hat{R} \equiv \{\theta, \varphi\}$.

For the application of the DWBA method, we write the interaction as $V(\mathbf{R}, \xi) = V_0(R) + W(\mathbf{R}, \xi)$ with

$$V_0(R) = \frac{\kappa Z_t Z_p e^2}{R} \tag{3.26}$$

and

$$W(\mathbf{R}, \xi) = \kappa Z_t e \sum_{\lambda>0,\mu} \frac{4\pi}{2\lambda+1} M(E\lambda, \mu) \frac{Y^*_{\lambda\mu}(\hat{R})}{R^{\lambda+1}} \tag{3.27}$$

The term $V_0(R)$ is just the usual monopole ($\lambda = 0$) Coulomb potential. This term does not depend on the internal coordinates of the projectile and hence cannot induce excitations. We can use the results of the preceding section, and calculate the scattering amplitude corresponding to the transition from an initial state ϕ_i to a final state ϕ_f. According to Eq. (3.20), we need to calculate matrix elements between initial and final states (i.e., the transition potentials). It is convenient to express the eigenstates of the internal Hamiltonian in terms of their angular momentum (I) and their projection (M), i.e.

$$|\phi_i\rangle \equiv |i; I_i M_i\rangle, \qquad |\phi_f\rangle \equiv |f; I_f M_f\rangle \tag{3.28}$$

so the transition potentials (3.21) result

$$W_{if}(\mathbf{R}) = \kappa Z_t e \sum_{\lambda\neq 0,\mu} \frac{4\pi}{2\lambda+1}\langle f; I_f M_f|M(E\lambda,\mu)|i; I_i M_i\rangle \frac{Y^*_{\lambda\mu}(\hat{R})}{R^{\lambda+1}} \tag{3.29}$$

Substituting this expression into the DWBA amplitude (3.20) we get

$$\begin{aligned} f(\theta)_{iM_i\to fM_f} = &-\frac{\mu}{2\pi\hbar^2}\kappa Z_t e \frac{4\pi}{2\lambda+1}\langle f; I_f M_f|M(E\lambda,\mu)|i I_i M_i\rangle \\ &\times \int d\mathbf{R}\chi_f^{(-)*}(\mathbf{K}_f,\mathbf{R})\frac{Y^*_{\lambda\mu}(\hat{R})}{R^{\lambda+1}}\chi_i^{(+)}(\mathbf{K}_i,\mathbf{R}) \end{aligned} \tag{3.30}$$

(recall that θ is the angle between $\mathbf{K}_i$ and $\mathbf{K}_f$)

If we define

$$\mathcal{T}^{\lambda}_{if}(\mathbf{K}_f,\mathbf{K}_i) \equiv \int d\mathbf{R}\chi_f^{(-)*}(\mathbf{K}_f,\mathbf{R})\frac{Y^*_{\lambda\mu}(\hat{R})}{R^{\lambda+1}}\chi_i^{(+)}(\mathbf{K}_i,\mathbf{R}) \tag{3.31}$$

we can rewrite the DWBA amplitude as

$$\boxed{f^{\mathrm{DWBA}}(\theta)_{iI_iM_i\to fI_fM_f} = -\frac{\mu}{2\pi\hbar^2}\kappa Z_t e\langle f; I_f M_f|M(E\lambda,\mu)|i; I_i M_i\rangle \mathcal{T}^{\lambda}_{if}(\mathbf{K}_f,\mathbf{K}_i)} \tag{3.32}$$

This result shows that the DWBA scattering amplitude factorizes into a product of two terms; the *amplitude* $\mathcal{T}^{\lambda}_{if}(\mathbf{K}_f,\mathbf{K}_i)$, which contains information on the *reaction* part, but does not depend on the specific structure of the projectile or target, and the structure factor $\langle f; I_f M_f|M(E\lambda,\mu)|i; I_i M_i\rangle$, which contains all the information on the nucleus being excited. This factorization makes it possible the extraction of structure information by comparing the angular and energy distributions of the outgoing nuclei with the DWBA calculation, provided that the approximations that lead to the DWBA result are valid.

The differential cross section will be given by,

$$\left(\frac{d\sigma}{d\Omega}\right)_{iM_i\to fM_f} = \frac{K_f}{K_i}\left|f(\theta)_{iM_i\to fM_f}\right|^2 . \tag{3.33}$$

This expression corresponds to a process in which the projectile is initially in a state with spin I_i and projection M_i and is excited to a state with spin I_f and projection M_f. In many experiments, the spin projection is not measured in either the initial nor the final states. In this case, the cross section is obtained averaging over the initial spin orientations and summing over their final orientations. If the spins are randomly oriented initially,

$$\left(\frac{d\sigma}{d\Omega}\right)_{i\to f} = \frac{1}{2I_i+1}\frac{K_f}{K_i}\sum_{M_i,M_f}\left|f(\theta)_{iM_i\to fM_f}\right|^2 . \tag{3.34}$$

It can be shown that this result is independent of the azimuthal angle φ.

The matrix elements of the electric multipole operator appearing in Eq. (3.32) can be expressed, using the Wigner-Eckart theorem, in terms of the reduced matrix elements as [8]

$$\langle f; I_f M_f | M(E\lambda,\mu) | i; I_i M_i \rangle = \langle I_f M_f | \lambda\mu I_i M_i \rangle \langle f; I_f || M(E\lambda) || i; I_i \rangle_{\rm BS} \,, \tag{3.35}$$

where the quantity $\langle f; I_f || M(E\lambda) || i; I_i \rangle$ is referred to as a *reduced matrix element*. It does not depend on the projections M_i and M_j. In the case of the electric operator, this is related to the **reduced transition probability**:[7]

$$B(E\lambda; i \to f) \equiv \frac{2I_f+1}{2I_i+1} |\langle f; I_f || M(E\lambda) || i; I_i \rangle_{\rm BS}|^2 \tag{3.36}$$

For a inelastic excitation $i \to f$ of multipolarity λ the differential cross section is proportional to the electric reduced probability $B(E\lambda; I_i \to I_f)$ because

$$\left(\frac{d\sigma}{d\Omega}\right)_{i\to f} \propto |\langle f; I_f || M(E\lambda) || i; I_i \rangle|^2 \propto B(E\lambda; I_i \to I_f)$$

So, if the approximations involved in the derivation of the DWBA amplitude are valid, the transition probabilities $B(E\lambda; I_f \to I_f)$ can be obtained comparing the magnitude of the inelastic cross sections with DWBA calculations. Note that the Clebsch-Gordan coefficient in Eq. (3.35) imposes certain restrictions with respect to the allowed transitions for a multipolarity λ, since this coefficient will be zero unless $|I_i - I_f| \le \lambda \le I_i + I_f$.

3.4.2 Nuclear excitation in the collective model

Within a collective model (e.g. vibrational, rotational,...) nuclear excitations are interpreted in terms of the deformation of the charge or mass distribution of the nucleus.

The interaction of a nucleus with a particle is typically characterized by a function of the distance from the particle to the nuclear surface (see Fig. 3.7). This is the case, for example, of the popular Woods-Saxon parametrization,

$$U_{\rm nuc}(R) = V(R-R_0) = -\frac{V_0}{1+\exp\left(\frac{R-R_0}{a_r}\right)} - i\frac{W_0}{1+\exp\left(\frac{R-R_i}{a_i}\right)}.$$

For a spherical nucleus, the interaction is of course independent on the orientation of the nucleus. However, if the nucleus is deformed (rotational nucleus) or can experience

[7] If the convention of reduced matrix elements of Bohr and Mottelson is used [7], the reduced matrix elements are defined as

$$\langle f; I_f M_f | M(E\lambda,\mu) | i; I_i M_i \rangle = (2I_f+1)^{1/2} \langle I_f M_f | \lambda\mu I_i M_i \rangle \langle f; I_f || M(E\lambda) || i; I_i \rangle_{\rm BM}$$

and hence, for the electric transition probability, we have

$$B(E\lambda; i \to f) \equiv \frac{1}{2I_i+1} |\langle f; I_f || M(E\lambda) || i; I_i \rangle_{\rm BM}|^2$$

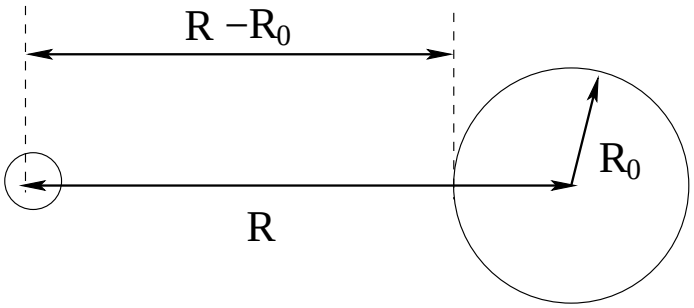

Figure 3.7: Interaction of a particle with a nucleus.

oscillations with respect to the spherical shape (vibrational nucleus), then the radius will have a dependence on the angles θ and φ (see appendix A.1):

$$r(\theta,\varphi) = R_0 + \sum_{\lambda,\mu} \hat{\delta}_{\lambda\mu} Y^*_{\lambda\mu}(\theta,\varphi) \tag{3.37}$$

where $\hat{\delta}_{\lambda\mu}$ are the so-called *deformation length operators* and characterize the deviation of the radius of the surface with respect to the spherical shape. Typically, the quadrupole ($\lambda = 2$) and octupole ($\lambda = 3$) deformations are the most relevant.

If we assume that the interaction with the reference particle is a function of the distance to the surface, we have:

$$V(\mathbf{R},\xi) = V(R - r(\theta,\varphi)) = V(R - (R_0 + \sum_{\lambda,\mu} \hat{\delta}_{\lambda\mu} Y^*_{\lambda\mu}(\theta,\varphi))) \tag{3.38}$$

Assuming that the deformation is small compared with the variation of the potential (eg. the diffuseness), we can perform a Taylor expansion of the potential in $\hat{\delta}_{\lambda\mu}$ which, up to first order, gives

$$V(\mathbf{R},\xi) = V(R - R_0) - \sum_{\lambda,\mu} \hat{\delta}_{\lambda\mu} \frac{dV(R-R_0)}{dR} Y^*_{\lambda\mu}(\theta,\varphi) + \ldots \tag{3.39}$$

To apply the DWBA formalism, we write the full interaction as $V = U + (V - U)$; we identify the second term with the residual interaction $W = V - U$, and the first term with the auxiliary potential U. The coupling potentials of the residual interaction between states $|i; I_i M_i\rangle$ and $|f; I_f M_f\rangle$ are [see Eq.(3.21)]:

$$W_{if}(\mathbf{R}) \equiv \langle f; I_f M_f | V | i; I_i M_i \rangle = -\frac{dV_0(R-R_0)}{dR} \sum_{\lambda,\mu} \langle f; I_f M_f | \hat{\delta}_{\lambda\mu} | i; I_i M_i \rangle Y^*_{\lambda\mu}(\hat{R}) \tag{3.40}$$

Inserting these transition potentials in the general expression for the DWBA amplitude

one gets:

$$f_{f,i}(\theta) = -\frac{\mu}{2\pi\hbar^2}\langle f; I_f M_f|\hat{\delta}_{\lambda\mu}|i; I_i M_i\rangle \times \int d\mathbf{R}\chi_f^{(-)*}(\mathbf{K}_f, \mathbf{R})\frac{dV}{dR}Y^*_{\lambda\mu}(\theta,\varphi)\chi_i^{(+)}(\mathbf{K}_i, \mathbf{R}) \tag{3.41}$$

As we did for the Coulomb case, this expression can be rewritten in a more compact form as:

$$\boxed{f_{fi}(\theta) = -\frac{\mu}{2\pi\hbar^2}\langle f; I_f M_f|\hat{\delta}_{\lambda\mu}|i; I_i M_i\rangle \mathcal{T}^{\lambda}_{i\to f}(\mathbf{K}_f, \mathbf{K}_i)} \tag{3.42}$$

with

$$\mathcal{T}^{\lambda}_{i\to f}(\mathbf{K}_f, \mathbf{K}_i) \equiv \int d\mathbf{R}\chi_f^{(-)*}(\mathbf{K}_f, \mathbf{R})\frac{dV_0}{dR}Y^*_{\lambda\mu}(\theta,\varphi)\chi_i^{(+)}(\mathbf{K}_i, \mathbf{R}) \tag{3.43}$$

And, for the differential cross section [c.f. (3.33)],:

$$\left(\frac{d\sigma(\theta)}{d\Omega}\right)_{iM_i\to fM_f} = \left(\frac{\mu}{2\pi\hbar^2}\right)^2 \frac{K_f}{K_i}\left|\langle f; I_f M_f|\hat{\delta}_{\lambda\mu}|i; I_i M_i\rangle\right|^2 \times \left|\int d\mathbf{R}\chi_f^{(-)*}(\mathbf{K}_f, \mathbf{R})\frac{dV_0}{dR}Y^*_{\lambda\mu}(\theta,\varphi)\chi_i^{(+)}(\mathbf{K}_i, \mathbf{R})\right|^2 \tag{3.44}$$

or, in terms of $\mathcal{T}^{\lambda}_{i\to f}$

$$\boxed{\left(\frac{d\sigma(\theta)}{d\Omega}\right)_{iM_i\to fM_f} = \left(\frac{\mu}{2\pi\hbar^2}\right)^2 \frac{K_f}{K_i}\left|\langle f; I_f M_f|\hat{\delta}_{\lambda\mu}|i; I_i M_i\rangle\right|^2 |\mathcal{T}^{\lambda}_{i\to f}(\mathbf{K}_f, \mathbf{K}_i)|^2} \tag{3.45}$$

The matrix elements of the deformation operators can be expressed in terms of a Clebsch-Gordan coefficient and a *reduced matrix element* (Wigner-Eckart theorem):

$$\langle f; I_f M_f|\hat{\delta}_{\lambda\mu}|i; I_i M_i\rangle = \langle f; I_f M_f|\lambda\mu I_i M_i\rangle\langle f; I_f\|\hat{\delta}_{\lambda}\|i; I_i\rangle_{\mathrm{BS}}. \tag{3.46}$$

When inserted into Eq. (3.44), we see that the differential cross section is proportional to the square of the reduced matrix elements $\langle f; I_f\|\hat{\delta}_{\lambda}\|i; I_i\rangle$ which, in turn, are related to the structure of the deformed nucleus. Consequently, if the approximations which lead to the DWBA are fulfilled, the comparison of experimental data on inelastic nuclear excitation of a nucleus provides information on its structure, for example, on its deviation of its shape from the spherical one.

In the particular case of the rotational model (see Appendix A.1) the deformation operator is given by:

$$\hat{\delta}_{\lambda\mu} = \beta_\lambda R_0 \mathcal{D}^{\lambda}_{\mu 0}(\omega) = \beta_2 R_0\sqrt{\frac{4\pi}{2\lambda+1}}Y_{\lambda\mu}(\theta_0, \phi_0), \tag{3.47}$$

where $\mathcal{D}$ stands for a rotation matrix and ω is the set of Euler angles (α, β, γ) corresponding to the transformation of the symmetry axis of the rotor to the laboratory frame.

In general, $\mathcal{D}$ depends on three indexes but, in the case of a axially symmetric rotor, one of the indexes is zero. In this case, $\mathcal{D}$ is given by a spherical harmonic, as indicated by the second equality of the previous equation. The rotor states are characterized in the rotor model by the total angular momentum (I), its projection along the z axis of the laboratory frame (M) and the projection of I along the symmetry axis (K). State with the same value of K belong to the same rotational band. A pure rotational excitation can change the value of I, but conserves K, that is, rotational excitations occur among states of a given rotational band. Using the results of Appendix A.1, the corresponding reduced matrix elements of $\hat{\delta}_{\lambda\mu}$ between these rotor states are given by[8]

$$\langle f; I_f \| \hat{\delta}_\lambda \| i; I_i \rangle_{\rm BS} = (-1)^{I_f - I_i} \langle I_f K \lambda 0 | I_i K \rangle \beta_\lambda R_0. \tag{3.49}$$

3.4.3 Simultaneous Coulomb and nuclear excitations

So far, we have considered separately the Coulomb and nuclear excitations. In some situations neglecting one of the interactions is justified. For example, we expect Coulomb excitation to be dominant when

- The projectile and/or target charges are large (i.e. large $Z_p Z_t \gg 1$)
- At energies well below the Coulomb barrier (where nuclear effects are less important).
- At very forward angles (large impact parameters).

However, in other cases, both Coulomb and nuclear contributions can be important and so the scattering amplitudes for both processes should be added *coherently*:

$$\left(\frac{d\sigma}{d\Omega}\right)_{i\to f} = \frac{K_f}{K_i} \left| f_{if}^{\rm coul} + f_{if}^{\rm nucl} \right|^2 \tag{3.50}$$

Note that, in this situation, interference effects will appear, making more delicate the extraction of structure information.

3.5 Example: ^{16}O $+^{208}$ Pb inelastic scattering

As an example, we consider the inelastic scattering of ^{16}O+^{208}Pb at energies around the Coulomb barrier, populating the low-lying states 3^- and 2^+ in ^{208}Pb [27].

[8] For the Bohr-Mottelson convention of reduced matrix elements:

$$\langle f; I_f \| \hat{\delta}_\lambda \| i; I_i \rangle_{\rm BM} = (-1)^{I_f - I_i} \sqrt{2I_f + 1} \langle I_f K \lambda 0 | I_i K \rangle \beta_\lambda R_0 \tag{3.48}$$

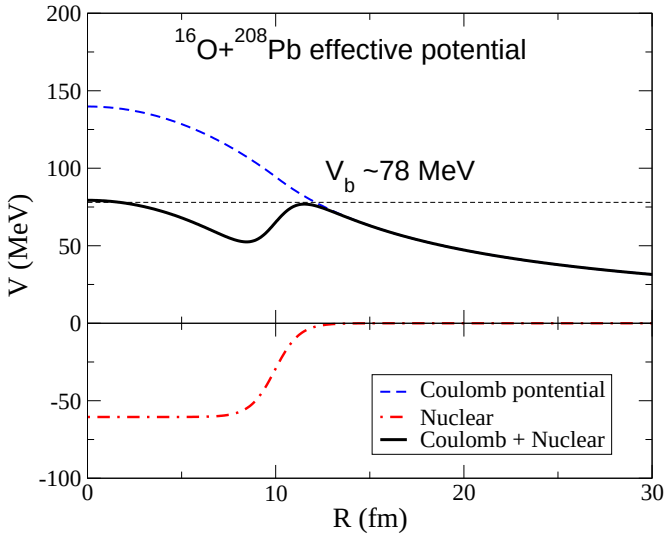

Figure 3.8: Effective (nuclear + Coulomb) potential for the ^{16}O+^{208}Pb system.

Using the nuclear potential from Ref. [27] the effective potential is as shown in Fig. 3.8. The energy of the Coulomb barrier, defined as the maximum of this effective potential, is slightly above 75 MeV. This is consistent with the simple estimate

$$V_{\rm barrier} \approx \frac{Z_p Z_t e^2}{1.44(A_p^{1/3} + A_t^{1/3})} \simeq 78 \text{ MeV}$$

So, for incident energies below 78 MeV, we expect that the Coulomb effects dominate, whereas above this energy nuclear effects will start to contribute too.

In Fig. 3.9 we show the experimental elastic and inelastic cross section angular distributions, taken from Ref. [27]. The elastic angular distribution (left panel) has been divided by the Rutherford cross section to make more clear the effect of the nuclear interaction and higher order ($\lambda > 0$) Coulomb effects. We see that, for energies well below the barrier, this relative angular distribution is one at all angles, meaning that the scattering is governed by the monopole Coulomb interaction ($V_C(r) = \kappa e^2 Z_p Z_t / r$). As the incident energy approaches the barrier, a reduction of the cross section is observed at the largest scattering angles, whereas at small angles it remains close to one. This can be understood in a classical picture. Classically, the smaller angles correspond to large impact parameters and hence to distant collisions. For these trajectories, the projectile *feels* only the Coulomb interaction, due to the short-range nuclear interaction. At large angles (small impact parameters) the classical turning point occurs at a small distance, and there is more chance to probe the nuclear interaction. As the bombarding energy increases above the barrier, these nuclear effects become more and more important, and the deviation from the Rutherford formula is more evident.

For the inelastic angular distributions we see also a evolution as the incident energy increases from the sub-barrier to the above-barrier regime. For energies below the barrier,

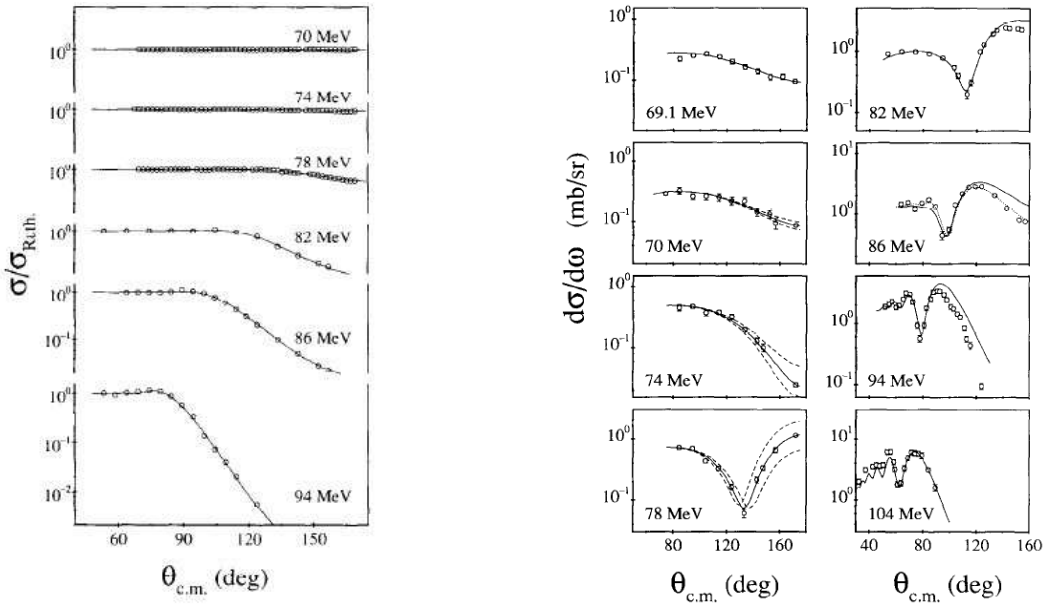

Figure 3.9: Experimental angular distribution for the elastic (left) and inelastic (right) cross section for the ^{16}O+^{208}Pb reaction for several incident energies. Quoted from [27].

the angular distribution is relatively featureless (at least for the angles displayed). Around and above the barrier, the distributions start to develop a deep minimum, and a more complicate pattern arises.

We try now to understand this behavior comparing the data with theoretical calculations, using the DWBA formalism discussed above. We assume that the DWBA is valid, and that the population of the 3^- state of the ^{208}Pb nucleus can be treated as an octupole collective excitation. We include both nuclear and Coulomb excitations. The corresponding DWBA amplitudes are given by Eqs. (3.30) and (3.41), respectively. The required physical ingredients are the reduced matrix elements $\langle f; I_f||M(E3)||i; I_i\rangle$ (for the Coulomb part) and $\langle f; I_f||\delta_3||i; I_i\rangle$ (for the nuclear part). The former can be obtained from the experimental value of the electric transition probability $B(E3; 0^+ \to 3^-) = 0.595\ \mathrm{e^2b^3}$. The reduced matrix element for the nuclear part was taken from the DWBA analysis of Ref. [27].

The calculated angular distributions are shown in Fig. 3.10 for $E_{\rm lab} = 69$ MeV and 82 MeV. The dashed and dot-dashed lines are the DWBA calculations for pure Coulomb and nuclear excitations, whereas the solid line is the coherent superposition of nuclear and Coulomb excitation. We see that at $E_{\rm lab} = 69$ MeV (below the barrier) the data can be mostly explained in terms of the Coulomb excitation. Nuclear excitation is very small at all angles, except at the largest angles, where it interferes destructively with the Coulomb amplitude. At $E_{\rm lab} = 82$ MeV, Coulomb couplings still dominate the smaller angles, but nuclear couplings are of the same order and even larger close to $\theta_{\rm c.m.} = 180°$. At $\theta_{\rm c.m.} \approx 140°$, there is a strong interference between both mechanisms, producing the minimum observed in the data.

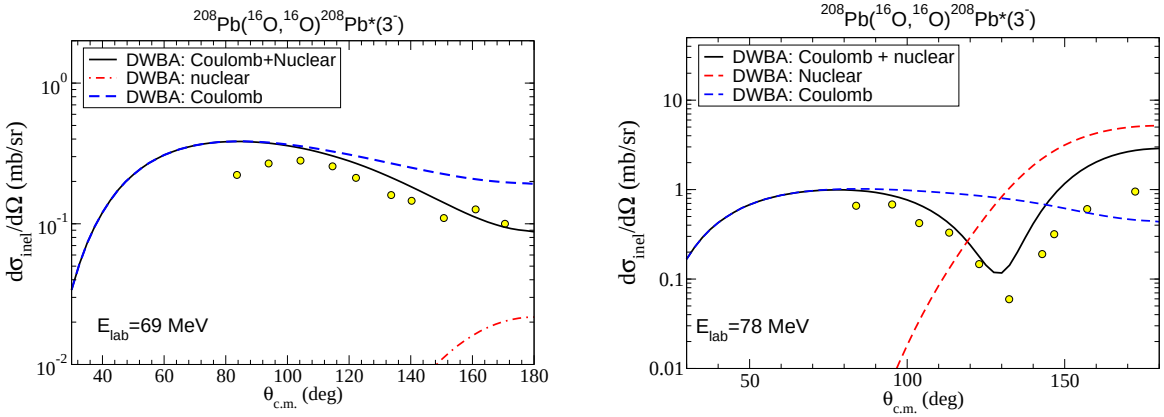

Figure 3.10: Experimental angular distribution for the population of the 3^- excited state in ^{208}Pb in the the ^{16}O+^{208}Pb reaction at an incident energy of 69 MeV (left) and 78 MeV (right) compared with DWBA calculations.

We see that a comparison of the data with the appropriate theory can provide useful information about the structure of the colliding nuclei and the mechanisms that take place in the reaction.

Chapter 4

Transfer reactions: the DWBA method

4.1 Introduction

A transfer reaction is another example of direct process. In this case, one or more nucleons of one of the colliding nuclei are transferred to the other nucleus. Historically, one uses the term *stripping* when nucleons are transferred from the projectile to the target, and *pick-up* when the nucleons are transferred from the target to the projectile. The prototypes of these reactions are the deuteron stripping reactions – denoted (d, p) and (d, n) – and their pick-up counter-parts (p, d) and (n, d).

4.2 Energy balance considerations

Let us denote generically a (binary) transfer reaction as:

$$a + A \to b + B$$

In the CM frame, the energy balance for this reaction is

$$E^i_{\rm cm} + M_a c^2 + M_A c^2 = E^f_{\rm cm} + M_b c^2 + M_B c^2 \tag{4.1}$$

Introducing the Q_0 value, defined in the same way as we did in the case of inelastic scattering (section 3.2),

$$\boxed{Q_0 = M_a c^2 + M_A c^2 - M_b c^2 - M_B c^2,}$$

the energy balance is rewritten as

$$E^f_{\rm cm} = E^i_{\rm cm} + Q_0 \tag{4.2}$$

Depending on the sign of Q_0, we have two distinct situations:

- $Q_0 > 0$: the system gains kinetic energy (exothermic reaction)

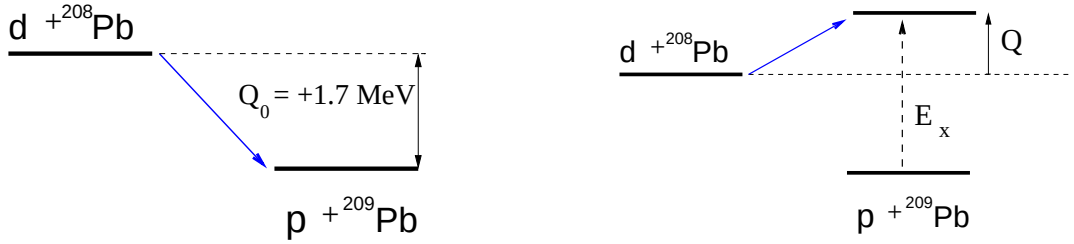

Figure 4.1: Illustration of the Q-value in the ^{208}Pb(d,p)^{209}Pb stripping reaction for a transfer to the ground state (left) and to an excited state (right) of the residual nucleus.

- $Q_0 < 0$: the system loses kinetic energy (endothermic reaction)

As an example, we consider the deuteron stripping reaction:

$$d + {}^{208}\mathrm{Pb} \rightarrow p + {}^{209}\mathrm{Pb}$$

In this case:

$$Q_0 = M_d c^2 + M(^{208}\mathrm{Pb})c^2 - M_p c^2 - M(^{209}\mathrm{Pb})c^2 = +1.7\,\mathrm{MeV}$$

so this corresponds to an exothermic reaction. This means that the outgoing proton will gain energy with respect to the incident deuteron. The energy balance is schematically depicted in Fig. 4.1(left).

Note that the difference $M(^{208}\mathrm{Pb})c^2 + M(1n)c^2 - M(^{209}\mathrm{Pb})c^2$ is just the one-neutron separation energy of ^{209}Pb. Analogously, $M_p + M_n - M_d$ is just the deuteron separation energy. Consequently, the Q-value can be interpreted (and calculated) also as the difference between the separation energy of the transferred particle(s) in the final and initial nuclei. In the previous example:

$$Q_0 = S_n(f) - S_n(i) = 3.936 - 2.224 = +1.7\ \mathrm{MeV}$$

So far, we have considered that the outgoing nuclei are left in their ground-state. Indeed, this is not necessarily the case and both the ejectile (that is, the fragment coming from the projectile) and the residual nucleus (the one coming from the target) can be left in an excited state. In this case, the energy balance should take into account the excitation energy of the final nuclei.

$$\boxed{E^f_{\mathrm{cm}} = E^i_{\mathrm{cm}} + Q = E^i_{\mathrm{cm}} + Q_0 - E_x} \tag{4.3}$$

where E_x denotes the excitation energy of the excited nucleus. In Fig. 4.1 (right) we illustrate the energy balance in the ^{208}Pb(d,p)^{209}Pb reaction, in which the transferred neutron populates an excited state of the residual nucleus ^{209}Pb.

In general, the residual nucleus will contain a number of bound excited states, which can be populated during the transfer reaction. According to Eq. (4.3), the excitation energy of the outgoing nuclei is directly related to their kinetic energy. So, for example, in

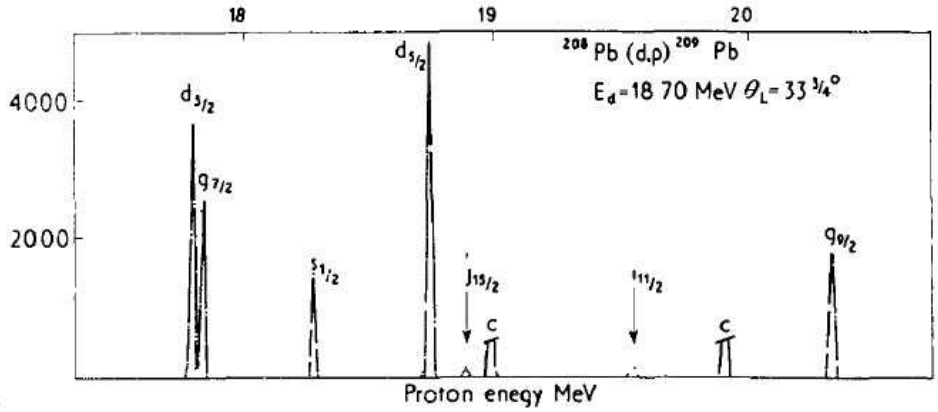

Figure 4.2: Proton energy in the reaction ^{208}Pb(d,p)^{209}Pb measured with a deuteron beam at 18.7 MeV and for a fixed proton scattering angle of 33°.

the ^{208}Pb(d,p)^{209}Pb example, the kinetic energy of the outgoing proton gives information about the energy spectrum of the ^{209}Pb nucleus[1]. This is shown in Fig. 4.2, which corresponds to the number of protons detected in a real ^{208}Pb(d,p)^{209}Pb reaction, as a function of its kinetic energy, for a given scattering angle. The peaks correspond to excited states of the ^{209}Pb nucleus. The labels accompanying each peak are single-particle quantum numbers assigned according to a simple independent particle model.

In the spectrum shown in Fig. 4.2, we see also that not all states are populated with the same intensity. The population probability will depend on the *reaction* dynamics as well as and on the *structure* properties of these states. Furthermore, transfer reactions can be used to infer *spectroscopic* information of the colliding nuclei, such as the intrinsic spin and parity of the populated states. The excitation spectrum by itself does not provide in general enough information to extract these properties. This information is usually obtained from the angular distribution of the outgoing ejectile. In order to extract useful physical information, these angular distributions must be compared with a suitable reaction theory, as we will see below.

4.3 The DWBA method

We want to derive a formal expression for the differential cross section corresponding to the transfer process (see Fig. 4.3)

$$\underbrace{(a+v)}_{A} + b \rightarrow a + \underbrace{(b+v)}_{B}.$$

Under the assumption that the transfer coupling is *small* with respect to the elastic

[1]Note that, in this particular example, the target is much more massive than the projectile and hence the laboratory energy of the proton will not differ much from its energy in the CM frame.

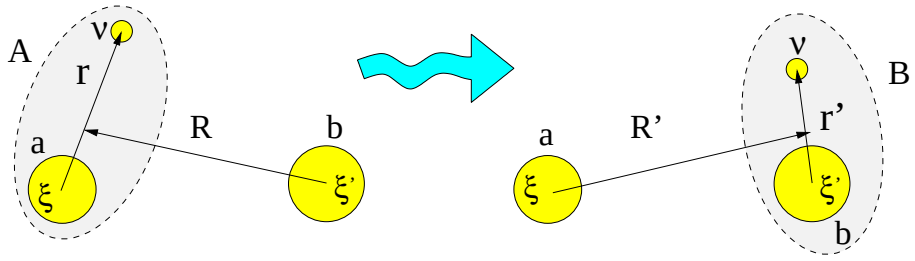

Figure 4.3: Post and prior representations for a transfer reaction

channel, we will describe this process using DWBA approximation, which was derived in Chapter 1 and was applied in Chapter 3 to the case of inelastic scattering.

In the case of transfer reactions, a similar expression can be derived, but the following differences need to be taken into account:

1. The projectile-target coordinate ($\mathbf{R}$) is different now in the initial and final channels, because they refer to different mass partitions. To distinguish between them we will use the notation $\mathbf{R}$ and $\mathbf{R}'$ (see Fig. 4.3).

2. The effective Hamiltonian is also different in the initial and final channels. Depending on whether we use the interactions for the initial or final channels we will use the names *prior* and *post*.

We start from the exact scattering amplitude derived in Chapter 1 using the Gell-Mann–Goldberger formula. The projectile–target interaction in the final partition (V_β) is expressed as $U_\beta + (V_\beta - U_\beta)$, where $U_\beta(\mathbf{R}_\beta)$ is some arbitrary potential. The exact scattering amplitude can be written as [c.f. Eq. (1.23)]:

$$\mathcal{T}_{\beta,\alpha} = \mathcal{T}^{(0)}_{\beta,\alpha}\delta_{\alpha\beta} + \int\int \chi^{(-)*}_\beta(\mathbf{K}_\beta, \mathbf{R}_\beta)\Phi^*_\beta(\xi_\beta)(V_\beta - U_\beta)\Psi^{(+)}_{\mathbf{K}_\alpha}(\mathbf{R}_\alpha, \xi_\alpha)d\xi_\beta d\mathbf{R}_\beta \quad , \tag{4.4}$$

Remember that the term $\mathcal{T}^{(0)}_{\beta,\alpha}$ corresponds to the scattering amplitude for an arbitrary potential U_β. By assumption, this potential does not depend on the internal coordinates of the projectile or target and, therefore, cannot contribute to inelastic scattering or transfer. Since we are interested in a transfer process, it can be dropped out. The distorted wave $\chi^{(-)}_\beta(\mathbf{K}_\beta, \mathbf{R}_\beta)$ is the time-reverse of $\chi^{(+)}(\mathbf{K}_\beta, \mathbf{R}_\beta)$, which describes the elastic scattering by the potential U_β.

The DWBA approximation is obtained approximating the total wavefunction $\Psi^{(+)}_{\mathbf{K}_\alpha}$ by

$$\Psi^{(+)}_{\mathbf{K}_\alpha}(\mathbf{R}_\alpha, \xi_\alpha) \approx \chi^{(+)}_\alpha(\mathbf{K}_\alpha, \mathbf{R}_\alpha)\Phi_\alpha(\xi_\alpha) \tag{4.5}$$

where $\Phi_\alpha(\xi_\alpha)$ is just the product of the internal states of the projectile and target ground-state wavefunctions. This gives rise to the DWBA approximation:

$$\mathcal{T}_{\beta,\alpha} = \int\int \chi_\beta^{(-)*}(\mathbf{K}_\beta, \mathbf{R}_\beta)\Phi_\beta^*(\xi_\beta)(V_\beta - U_\beta)\chi_\alpha^{(+)}(\mathbf{K}_\alpha, \mathbf{R}_\alpha)\Phi_\alpha(\xi_\alpha)d\xi_\beta d\mathbf{R}_\beta \quad . \tag{4.6}$$

The expressions (4.4) and (4.6) are known as *post* forms of the scattering amplitude, because they contain a matrix element of the residual interaction $V_\beta - U_\beta$ in the final channel. An analogous (and equivalent) *prior* form *exact* amplitude is given by ($\beta \neq \alpha$)

$$\mathcal{T}_{\beta,\alpha}^{\text{prior}} = \int\int \Psi_{\mathbf{K}_\beta}^{(-)*}(\mathbf{R}_\beta, \mathbf{r}_\beta)(V_\alpha - U_\alpha)\chi_\alpha^{(+)}(\mathbf{K}_\alpha, \mathbf{R}_\alpha)\Phi_\alpha(\xi_\alpha)d\xi_\alpha d\mathbf{R}_\alpha \quad , \tag{4.7}$$

where V_α is the projectile-target interaction in the initial partition, $U_\alpha(\mathbf{R}_\alpha)$ some arbitrary potential defined in the coordinate and $\chi_\alpha^{(+)}(\mathbf{K}_\alpha, \mathbf{R}_\alpha)$ a distorted wave describing the projectile-target motion under the potential $U_\alpha(\mathbf{R}_\alpha)$.

The prior DWBA approximation is obtained making the approximation

$$\Psi_{\mathbf{K}_\beta}^{(-)}(\mathbf{R}_\beta, \xi_\beta) \approx \chi_\beta^{(-)}(\mathbf{K}_\beta, \mathbf{R}_\beta)\Phi_\alpha(\xi_\alpha) \tag{4.8}$$

In the remaining of this chapter, we relax the notation by taking: $\mathbf{R}_\alpha \to \mathbf{R}$ and $\mathbf{R}_\beta \to \mathbf{R}'$. With this new notation, the relevant coordinates are shown in Fig. 4.3.

Even within the DWBA approximation, Eqs. (4.6) or (4.8) are difficult to solve, because they involve many-body wavefunctions of the initial and final nuclei ($\Phi_\alpha(\xi_\alpha)$ and $\Phi_\beta(\xi_\beta)$) and the projectile–target interactions (V_α and V_β). With some further approximations, we can reduce this complicate many-body problem to an effective three-body problem. First, we write the wavefunction $\Phi_\alpha(\xi_\alpha)$ as (see Fig. 4.3):

$$\Phi_\alpha(\xi_\alpha) = \Phi_A(\xi, \mathbf{r})\phi_b(\xi') \tag{4.9}$$

and the quantum mechanical state of the composite nucleus A is further expanded as

$$\Phi_A(\xi, \mathbf{r}) = C_{va}^A \phi_a(\xi)\phi_v\varphi_{av}(\mathbf{r}) + \Phi_A^C. \tag{4.10}$$

In this simplified notation, ϕ_a and ϕ_v represent the internal wavefunctions of clusters a and v, $C_{av}^A\varphi_{av}(\mathbf{r})$ represents the overlap function, which can be written in terms of a normalized relative wavefunction $\varphi_{av}(\mathbf{r})$ and a spectroscopic amplitude C_{av}^A. The product of these three terms is implicitly coupled to the angular momentum of nucleus A.

Notice that not all the state Φ_A can be described as two clusters b, v with a certain state of relative motion. Φ_A^C represents the part of the state that has a more complicated configuration.

Similarly, for the final partition, we may write

$$\Phi_\beta(\xi_\beta) = \Phi_B(\xi', \mathbf{r}')\phi_a(\xi) \tag{4.11}$$

and the state of the composite nucleus B is expanded as

$$\Phi_B(\xi', \mathbf{r}') = C_{vb}^B \phi_b(\xi')\phi_v\varphi_{bv}(\mathbf{r}') + \Phi_B^C. \tag{4.12}$$

The following approximations allow us to reduce the many-body problem to a three-body problem:

- The terms Φ_A^C and Φ_B^C, corresponding to complex configurations of A and B, do not contribute significantly to transfer and are therefore neglected.

- The normalized overlap functions $\varphi_{bv}(\mathbf{r}')$ and $\varphi_{av}(\mathbf{r})$ can be approximated by the eigenstates of two-body Hamiltonians with interactions V_{bv} and V_{av}, respectively. They will be represented by some real mean-field interactions.

- During the collision process the interactions between the clusters a,b, and v are completely described by two-body interactions V_{bv}, V_{av} and U_{ab}, that cannot alter the internal states of the clusters. In our description of transfer, we do not consider explicitly processes that lead to the excitations of the clusters b and a, so the interaction between them is represented by an effective optical potential, complex in general, that we denote by U_{ab}. So we will write:

$$V_\alpha - U_\alpha \to V_{bv} + U_{ab} - U_{bA} \equiv V_{\rm prior} \tag{4.13}$$
$$V_\beta - U_\beta \to V_{av} + U_{ab} - U_{aB} \equiv V_{\rm post}\ . \tag{4.14}$$

  The differences $U_{ab} - U_{bA}$ (in prior form) and $U_{ab} - U_{aB}$ (in post form) are called **remnant terms**. For a suitable choice of U_{bA} (prior) or U_{bA} (post) we can achieve some cancellation of these remnant terms and hence the transfer will be dominated by the valence–core interaction V_{bv} (prior) or V_{av} (post).

The corresponding transition amplitudes result:

$$\mathcal{T}^{\rm prior} \approx C_{bv}^{B*} C_{av}^{A} \mathcal{T}^{3b}_{\rm prior} \tag{4.15}$$
$$\mathcal{T}^{\rm post} \approx C_{bv}^{B*} C_{av}^{A} \mathcal{T}^{3b}_{\rm post} \tag{4.16}$$

with[2]

$$\mathcal{T}^{3b}_{\rm prior} = \int\int \chi_\beta^{(-)*}(\mathbf{K}',\mathbf{R}')\varphi^*_{bv}(\mathbf{r}')V_{\rm prior}\chi_\alpha^{(+)}(\mathbf{K},\mathbf{R})\varphi_{av}(\mathbf{r})d\mathbf{R}d\mathbf{r}. \tag{4.17}$$

and

$$\mathcal{T}^{3b}_{\rm post} = \int\int \chi_\beta^{(-)*}(\mathbf{K}',\mathbf{R}')\varphi^*_{bv}(\mathbf{r}')V_{\rm post}\chi_\alpha^{(+)}(\mathbf{K},\mathbf{R})\varphi_{av}(\mathbf{r})d\mathbf{R}'d\mathbf{r}'. \tag{4.18}$$

It can be formally demonstrated that the *prior* and *post* DWBA expressions give exactly the same result. Hence, the choice of one of another representation is done by computational convenience, determined by the range of the interactions. In many situations, an appropriate choice of the auxiliary potential produces a certain cancellation of the *remnant term*. In those situations, the transition amplitude is mostly determined by

[2]Note that, $d\xi_\beta = d\xi d\xi' d\mathbf{r}$. To evaluate the T-matrix, we have to perform integrals of the form

$$\int \Phi_B^*(\xi',\mathbf{r}')\Phi_b(\xi')d\xi' = C_{bv}^B\varphi_{bv}(\mathbf{r}').$$

where we have used the parentage decomposition of Φ_B^* in terms of b state (likewise for A).

the interaction V_{av} (post) or V_{bv} (prior) and it results numerically advantageous to choose the representation for which this interaction is of shorter range.

The accuracy of DWBA depends on the choice of the auxiliary potentials for the incident (U_{Ab}) and final (U_{aB}) channels. These could be, in principle, any function of the co-ordinate $\mathbf{R}$ and $\mathbf{R}'$, respectively. Two approaches are usually taken:

- *The microscopic approach.* The auxiliary potential in the outgoing channel U_{aB} is taken as the expectation value, in the final bound state $\varphi_{bv}(\mathbf{r}')$, of the sum of the interactions $U_{ab} + V_{va}$. Explicitly,

$$U_{aB}(\mathbf{R}') = \int d^3\mathbf{r}' \left|\varphi_{bv}(\mathbf{r}')\right|^2 (U_{ab} + V_{av}). \tag{4.19}$$

  Similarly, U_{Ab} is taken as the expectation value, in the initial bound state, of the sum of the interactions $U_{ab} + V_{vb}$,

$$U_{Ab}(\mathbf{R}) = \int d^3\mathbf{r} \left|\varphi_{av}(\mathbf{r})\right|^2 (U_{ab} + V_{bv}). \tag{4.20}$$

  In practical applications of DWBA, it is very convenient that the auxiliary potentials are central, so that they depend on the value of the radial co-ordinate $U_{Ab}(R), U_{aB}(R')$ and not in its direction. This is achieved considering only the monopole part of the folding interaction, or, equivalently, averaging the folding potential over all the magnetic substates.

  The microscopic approach has the advantage of being completely determined by the two-body interactions between the fragments. From the formal point of view, this would be the natural choice for U_{Ab}, in order to make the residual term $U_{ab}+V_{vb}-U_{Ab}$ minimal, for the bound state φ_{av}.

  On the negative side, it is not trivial that the interaction U_{Ab}, so obtained, would reproduce accurately the $A + b$ elastic scattering. The interactions U_{ab}, V_{av}, V_{bv} would have to be taken as complex interactions, in order to reproduce elastic scattering or transfer, but in this case V_{av}, V_{bv} can not be used to obtain bound states, unless the interactions are explicitly energy dependent. Finally, this approach excludes completely any effect of break-up channels on the three-body wavefunction. Hence, this approach would be valid when the three-body scattering wavefunctions is dominated by the elastic component, either in the incident or in the exit channels.

- *The phenomenological approach.* The auxiliary potential in the incident channel U_{Ab} is obtained by fitting the elastic scattering data on the α ($=A + b$) channel. The auxiliary potential in the exit channel, U_{aB}, is obtained by fitting the elastic scattering on the β ($= a + B$) channel. This approach has the advantage of allowing for a consistent description of transfer reactions, as well as of elastic scattering in the incident and outgoing channels. It takes into account, through the use of

optical potentials, the effect of complex reaction processes, such as fusion, that can remove flux from the elastic and from the transfer channels. Furthermore, the effect of some three-body reactions, such as break-up, which remove flux from elastic and transfer channels, are approximately taken into account because the optical potentials fit the experimental elastic cross sections, which are affected by all these dynamic processes. On the negative side, it is not always possible to find the elastic data for the outgoing channel. If the final state of nucleus B is not in its ground state, but on an excited state, it will not be possible to measure the corresponding elastic scattering. This is particularly true if the final state is in the continuum. Besides, the optical potentials reproduce typically the asymptotic wavefunctions, which determines the S-matrix and the scattering amplitudes leading to differential cross sections. It does not necessarily reproduce the wavefunctions in the internal radial range that is relevant for the transfer matrix elements.

Recalling the relation between the T-matrix and the scattering amplitude we have (prior form, likewise for post form)

$$\boxed{f^{\rm prior}_{\beta,\alpha}(\theta) = -\frac{\mu_\beta}{2\pi\hbar^2} C^{B*}_{bv} C^A_{av} \int\int \chi^{(-)*}_\beta(\mathbf{K}',\mathbf{R}')\varphi_{bv}(\mathbf{r}')V_{\rm prior}(\mathbf{R},\mathbf{r})\varphi_{av(\mathbf{r})}\chi^{(+)}_\alpha(\mathbf{K},\mathbf{R})d\mathbf{R}d\mathbf{r}} \tag{4.21}$$

and the corresponding differential cross section

$$\left(\frac{d\sigma_{\alpha,\beta}}{d\Omega}\right)^{\rm prior} = \frac{\mu_\alpha\mu_\beta}{(2\pi\hbar^2)^2}\frac{K_\beta}{K_\alpha}|C^B_{bv}|^2|C^A_{av}|^2 \times \left|\int\int \chi^{(-)*}_\beta(\mathbf{K}',\mathbf{R}')\varphi_{bv}(\mathbf{r}')V_{\rm prior}(\mathbf{R},\mathbf{r})\varphi_{av}(\mathbf{r})\chi^{(+)}_\alpha(\mathbf{K},\mathbf{R})d\mathbf{R}d\mathbf{r}\right|^2 \tag{4.22}$$

The factors $S^B_{\ell bv} = |C^B_{bv}|^2$ and $S^A_{av} = |C^B_{bv}|^2$ are called **spectroscopic factors**. The spectroscopic factor S^A_{av} can be regarded as the probability of finding the valence particle v in a given state $\varphi_{av}(\mathbf{r})$ coupled to the core in the state a. According to this result, in DWBA, the transfer cross section is proportional to the product of spectroscopic factors $S^B_{bv}\, S^A_{av}$. This is a very important and useful result because, whenever the approximations which lead to Eq. (4.22) are justified, we can extract information on the spectroscopic factors of the colliding nuclei by comparing the experimental data with the DWBA prediction.

Let us finish by summarizing the approximations and assumptions inherent to the DWBA method:

1. Only the transferred particle (or particles) is treated explicitly, while all the others, which we refer generically as the core, are regarded as passive or inert (the core is assumed to remain unchanged during the collision9

2. Assumes that the elastic optical potential U_α provides waves functions for the relative motion which are good within the range of the potential $V - U$. For example,

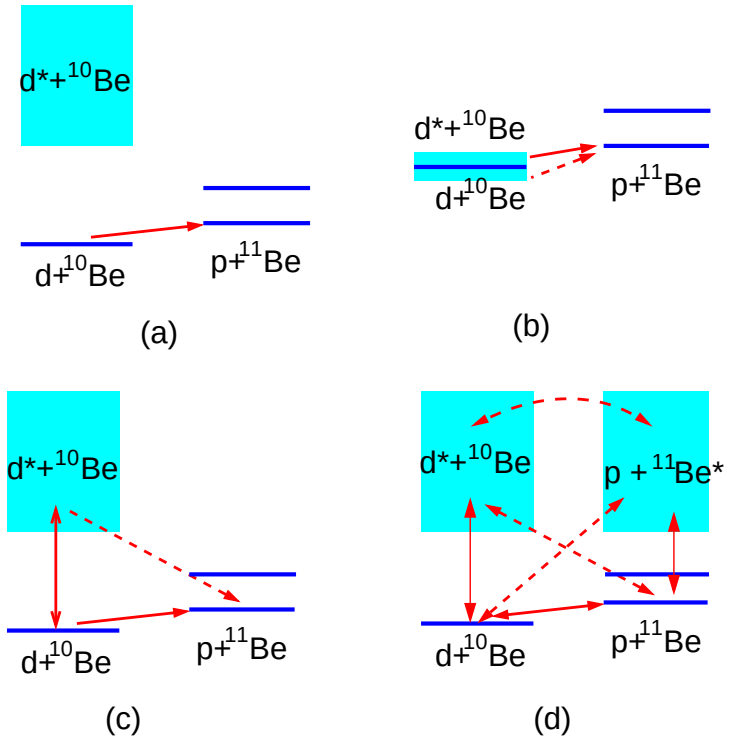

Figure 4.4: Comparison of different coupling schemes discussed in this work for the reaction ^{10}Be(d,p)^{11}Be: (a) DWBA, (b) CDCC-BA, (c) ADWA and (c) CRC.

for a (d, p) reaction in post form, $V_{\rm post} = V_\beta - U_\beta \approx V_{pn}$ and so the distorting potentials must be accurate for small $p - n$ separations.

3. Assumes that the transfer process is weak so that it can be treated in first order.

The coupling scheme assumed in the DWBA method is schematically depicted in Fig. 4.4(a) for the ^{10}Be(d,p)^{11}Be case. The solid arrow indicates that only transfer from the ground state of the deuteron to the proton channel is explicitly included. The effect of breakup channels of the deuteron (shaded area in this plot) is completely neglected in the afore-mentioned microscopic approach, and only partially taken into account in the phenomenological approach, through its effect on the elastic wavefunction.

Spins and antisymmetrization: spectroscopic factors

The quantities $|C^B_{bv}|^2$ and $|C^A_{av}|^2$ are called *spectroscopic factors*. Recalling (4.12) or (4.10), they give information on *finding* a given single-particle configuration in the composite system. So, for example, $|C^A_{av}|^2$, tell us the *probability* of finding the valence particle in the single-particle state $\varphi_{av}(\mathbf{r})$, coupled to the core a in some given state, to give the composite state A. We note here that our description is somewhat schematic, because (i) we have not introduced the spins explicitly and (ii) we have not considered antisymetrization, that is, the fact that the composite and core wavefunctions are described by antisymmetrized wavefunctions and that the transferred particle is indistinguishable from those of the same orbital in the donor or receptor nuclei. So, for example, the composite nucleus A would be characterized by some total angular momentum J and projection M. Its state should be described by a fully antisymmetrized wavefunction, $\Phi^{JM}_A(\xi,\mathbf{r})$. Analogously, the core nucleus B, will be characterized by a fully antisymmetrized wavefunction with angular momentum and projection I, M_I. It is possible to expand the wavefunction $\Phi^{JM}_A(\xi,\mathbf{r})$ in terms of products of valence and core configurations, i.e.,

$$\begin{aligned}\Phi^{JM}_A(\xi,\mathbf{r}) &= \frac{1}{\sqrt{n_A}}\sum_{I\ell j} C^{IJ}_{\ell sj}\left[\Phi^I_a(\xi)\otimes\varphi^{\ell sj}_{av}(\mathbf{r}\right]_{JM}\\ &= \frac{1}{\sqrt{n_A}}\sum_{I\ell j}\langle IM_I jm|JM\rangle C^{IJ}_{\ell sj}\Phi^{IM_I}_a(\xi)\varphi^{\ell sjm}_{av}(\mathbf{r})\end{aligned} \tag{4.23}$$

where n_A is the number of equivalent nucleons. This factor accounts for the antisymmetrization of the wavefunction since these n_A nucleons are indistinguishable. If the overlaps functions $\varphi^{\ell sjm}_{av}(\mathbf{r})$ are normalized to unity, the coefficients $C(A|a)^{IJ}_{\ell sj}$ are the **spectroscopic amplitudes** or **coefficients of fractional parentage**. Their square are the spectroscopic factors:

$$S^{IJ}_{\ell sj} = |C^{IJ}_{\ell sj}|^2 \tag{4.24}$$

The overlap wave functions $\varphi^{\ell sjm}_{av}(\mathbf{r})$ and $\varphi^{\ell sjm}_{bv}(\mathbf{r}')$ are not easy to calculate from microscopic structure models. For that reason, the standard procedure is to approximate these functions by the solutions of a one-body Schrödinger equation assuming a simple potential shape (typically, a Woods-Saxon shape), for the apropriate quantum numbers $\{n,l,s,j\}$, and the experimental separation energy

$$\left[-\frac{\hbar^2}{2\mu_{va}}\nabla^2_{\mathbf{r}} + V_{va}(\mathbf{r}) - \varepsilon_{va}\right]\varphi^{\ell sj}_{av}(\mathbf{r}) = 0\,, \tag{4.25}$$

and

$$\left[-\frac{\hbar^2}{2\mu_{vb}}\nabla^2_{\mathbf{r}} + V_{vb}(\mathbf{r}) - \varepsilon_{vb}\right]\varphi^{\ell sj}_{bv}(\mathbf{r}) = 0\,, \tag{4.26}$$

where ε_{va} and ε_{vb} are the binding energy of the valence particle in the nuclei A and B, respectively.

4.4 Examples and applications of the DWBA method

Dependence with the quantum numbers of the transferred particle

The DWBA does not only provide information on spectroscopic factors. The shape of the angular distribution obtained with Eq. (4.22) is found to depend critically on the internal wavefunctions $\varphi^A_{\ell sj}(\mathbf{r})$ and $\varphi^B_{\ell' sj'}(\mathbf{r}')$. If we have an accurate model for either the projectile or target (this is the case of a (d,p) reaction) then we can infer information on the other nucleus.

As an example we show in Fig. 4.5 several calculations for the ^{56}Fe$(d,p)^{57}$Fe reaction, each of them using a different choice for the orbital angular momentum of the transferred neutron in the final state.

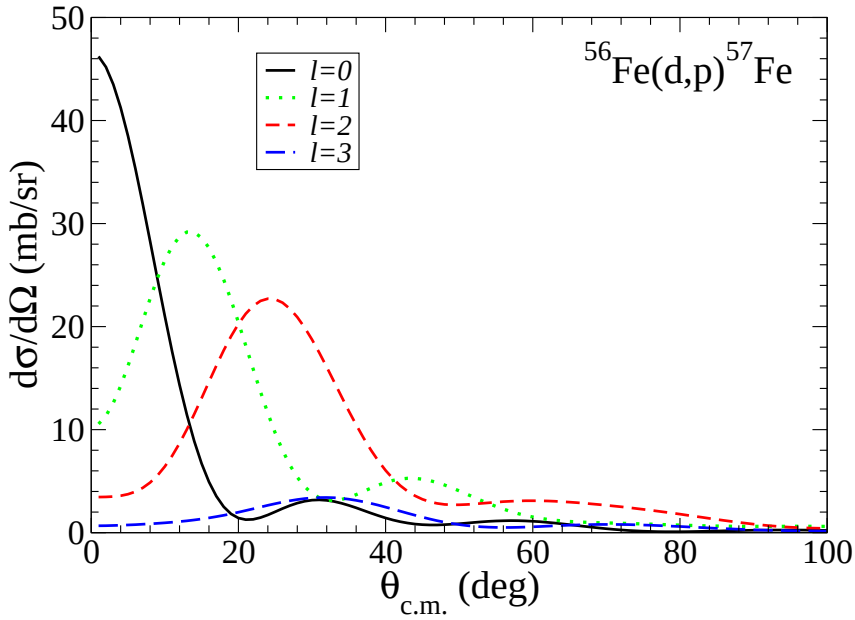

Figure 4.5: DWBA calculations for the differential cross section of the reaction ^{56}Fe$(d,p)^{57}$Fe, showing several assumptions for the wavefunction of the transferred neutron in the ^{57}Fe residual nucleus.

Dependence with the binding energy

In addition to the quantum numbers, the wavefunctions $\varphi^A_{\ell sj}(\mathbf{r})$ will depend on the binding energy of the transferred particle. This is illustrated in Fig. 4.6, where we show several DWBA calculations for a given single-particle configuration, and varying the binding energy of the transferred neutron in the final nucleus. The larger the separation energy, the smaller the cross section. This is expected since a more bound nucleon will be more difficult to remove than a weakly bound nucleon.

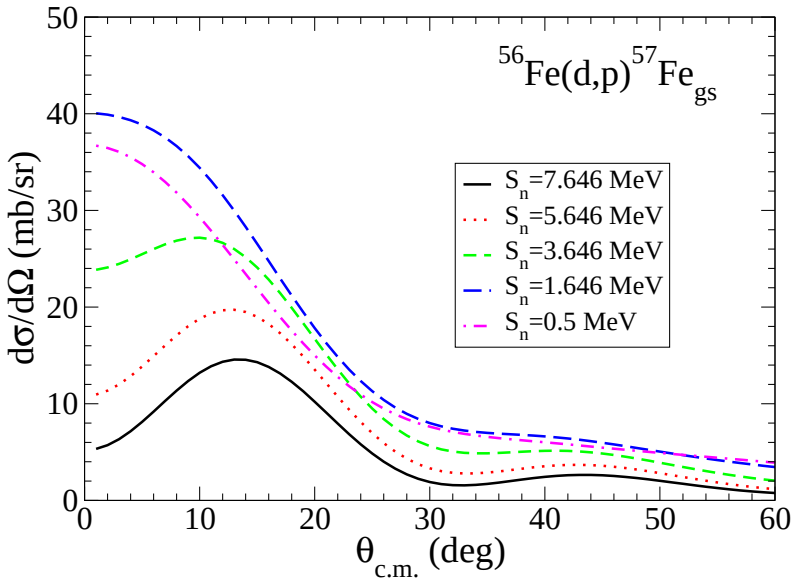

Figure 4.6: DWBA calculations for the differential cross section of the reaction ^{56}Fe(d,p)^{57}Fe, for a fixed configuration of the transferred neutron, and several values of its separation energy in the ^{57}Fe residual nucleus.

Dependence with the incident energy

In inelastic scattering, the excitation probability increases with the incident energy; the larger the incident energy, the larger the transferred momentum to the projectile or target. On the other hand, for transfer reactions there is an optimal energy for which the transfer occurs. This is shown in Fig. 4.7 for our working example, ^{56}Fe(d,p)^{57}Fe. In this case, the optimum energy is about 9 MeV (that is, about 4.5 MeV per nucleon).

4.5 Beyond DWBA: ADWA and CCBA methods

In general, DWBA has been, and still is, a key approach to describe transfer reactions, and it has been used extensively to extract spectroscopic information on nuclear structure, in particular spectroscopic amplitudes. However, DWBA is based on a rather crude approach to the three-body problem, and is expected to be accurate only when the elastic scattering, in the incident and outgoing channels, is dominant. For the case of exotic nuclei, which are frequently weakly bound, break-up channels can play a very important role in the three-body dynamics. Hence, it is important, in order to extract reliable spectroscopic information from transfer reactions with exotic nuclei, to check the validity of the DWBA method by comparing it with other approaches that take into account the role of break-up channels.

The DWBA approach, as mentioned previously, relies strongly on the assumption that the elastic channel dominates the reaction. This does not only imply that the dominant

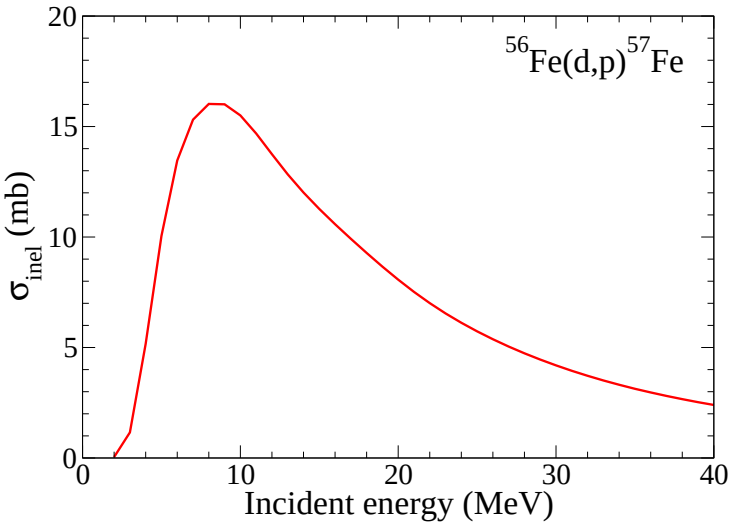

Figure 4.7: DWBA calculations for the differential cross section of the reaction ^{56}Fe(d,p)^{57}Fe as a function of the incident energy.

cross sections is elastic, but also that, during the collision process, the three-body wavefunction can be approximated by the elastic component. Note that these two facts are not equivalent. There can be dynamic situations in which elastic cross section dominates, meaning that the asymptotic three-body wavefunction, at large distances, is dominated by the elastic component. However, this does not mean that at short projectile-target distances, which give the main contribution to the transfer matrix element, the elastic component should be dominant. Dynamic polarization effects make that the composite projectile can be strongly distorted at short distances, even when asymptotically the energy matching conditions make the elastic channel dominant.

Moreover, the phenomenological DWBA approach relies on the use of optical potentials, usually taken as local, L-independent potentials, chosen to reproduce elastic scattering. This means that the optical potentials will reasonably reproduce the phase shifts, for all L-values, in the elastic channel. In other words, the phenomenological DWBA approach reproduces the elastic wavefunction asymptotically, at large projectile-target distances. It is not trivial that the elastic wavefunction used in the phenomenological DWBA approach reproduce correctly the elastic component of the wavefunction, in the radial range relevant for the transfer T-matrix elements.

We discuss in the next subsections some approaches that go beyond the DWBA method.

4.5.1 The adiabatic (ADWA) method

Indeed, this criticism of the DWBA approach is not very useful if an alternative formulation is available, which maintains the relative simplicity of DWBA, and provides

ingredients of the reaction calculation that can be completely determined from experiment. This is achieved by the Adiabatic Distorted Wave Approximation (ADWA), which was initially formulated by Johnson and Soper [16]. This approach is formulated in principle for (d,p), or (d,p) reactions, although it could be applied to other weakly bound composite systems. It relies on the fact that the composite projectile has a relatively low binding energy (2.22 MeV in the case of the deuteron), and so, if the collision energy is relatively high, we can expect that, during the collision process, the relative proton-neutron co-ordinate does not change significantly; it is "frozen". Under this situation, the relevant interaction that determines accurately the projectile-target wavefunction is not the phenomenological deuteron-target interaction that would reproduce elastic scattering, but the sum of the interactions of each one of the fragments of the projectile (proton and neutron in the deuteron case) with the target.

In the *adiabatic approximation* [16] (also called *sudden approximation* by some authors) the three-body wavefunction can be written as

$$\Psi^{(+)}_{\mathbf{K}}(\mathbf{R},\mathbf{r}) \simeq \chi^{(+)}_{\alpha}(\mathbf{K},\mathbf{R},\mathbf{r})\varphi_{av}(\mathbf{r}), \tag{4.27}$$

where $\chi^{(+)}_{\alpha}(\mathbf{R},\mathbf{r})$ is the solution of a two-body scattering problem, on the co-ordinate $\mathbf{R}$, in which the interaction is given by

$$U_{Ab}(\mathbf{R},\mathbf{r}) = U_{ab}(R_{ab}) + V_{vb}(r'). \tag{4.28}$$

Indeed, the potential that describes the scattering wavefunction, although two-body, is not central and so the calculation of the adiabatic wavefunction, for each value of the a-v separation $\mathbf{r}$ is very complicated, but it has been done [3, 4]. Besides, the adiabatic approximation to the three-body wavefunction is not accurate for large values of $\mathbf{r}$, where one would expect to see outgoing waves, instead of the exponential decay given by the bound two-body wavefunction $\varphi_{av}(\mathbf{r})$.

Fortunately, these shortcomings of the adiabatic wavefunctions are not important, if one is only interested in evaluating the matrix element involved in transfer. These are dominated by the $V_{av}(r)$ interaction (the proton-neutron interaction, in the deuteron case) which has a short range. Note that, even if the a-v wavefunction $\varphi_{av}(\mathbf{r})$ has a relatively long range, which is the case for weakly bound halo systems, the $V_{av}(r)$ has a much shorter range. Hence, for the purpose of evaluating the transfer matrix element, one can evaluate the adiabatic wavefunction using the potential evaluated at $\mathbf{r} = 0$. This leads to the Johnson and Soper approximation [16], in which

$$\Psi^{(+)}(\mathbf{R},\mathbf{r}) \simeq \chi^{(+)}_{\alpha}(\mathbf{K},\mathbf{R})\varphi_{av}(\mathbf{r}), \tag{4.29}$$

where $\chi^{(+)}_{\alpha}(\mathbf{K},\mathbf{R})$ is the solution of a two-body scattering problem, on the co-ordinate $\mathbf{R}$, in which the interaction is given by

$$U^{JS}_{Ab}(R) = U_{ab}(R) + U_{vb}(R). \tag{4.30}$$

Note that, in this expression, the $v-b$ interaction V_{vb}, which would in general be energy dependent, and would generate the bound state $\varphi_{bv}(\mathbf{r}')$, is replaced by the optical potential

U_{vb} that describes the $v-b$ interaction at the same energy per nucleon in the incident beam. This is justified by the adiabatic approximation; the transfer process dynamics is consistent with freezing the a-v co-ordinate, that then scatters from the b target with an interaction that is the sum of U_{bv} and U_{ba} interactions at the same energy per nucleon.

Several refinements and corrections have been performed to the ADWA formalism. For example, a finite-range version of the adiabatic potential was proposed by Johnson and Tandy [17]:

$$U_{Ab}^{JT}(R) = \frac{\langle \varphi_{av}(\mathbf{r}) | V_{av}(U_{ab} + U_{vb}) | \varphi_{av}(\mathbf{r}) \rangle}{\langle \phi_{av}(\mathbf{r}) | V_{av} | \phi_{av}(\mathbf{r}) \rangle} . \tag{4.31}$$

However, for the purpose of the analysis of (d,p) and (p,d) reactions, the simplest Johnson-Soper expression given by Eq. (4.30) is by far the most widely used. Here, we will outline its advantages and disadvantages. On the positive side, the ADWA approach ingredients are completely determined by experiments. These ingredients are the proton-target and neutron-target optical potentials, evaluated at half of the deuteron scattering energy, as well as the well known proton-neutron interaction.

The adiabatic approximation is equivalent to neglect the excitation energy of the states of the projectile [16]. The adiabatic wavefunction takes into account the excitation to breakup channels, but assuming that these states are degenerate in energy with the projectile ground state, as illustrated in Fig. 4.4(c). Therefore, the ADWA approach takes into account, approximately, the effect of deuteron break-up on the transfer cross section, within the adiabatic approximation. So, it should be well suited to describe deuteron scattering at high energies, around 100 MeV per nucleon. Systematic studies [13, 25, 30] have shown that ADWA is superior to standard DWBA for (d,p) scattering at high energies.

On the negative side, the ADWA approach does not consistently describe elastic scattering and transfer. Although physically one considers that elastic scattering, transfer and break-up should be closely related, so that the increase of flux in one channel should reduce the flux in the others, this connection is not present in ADWA. On the other hand, the arguments leading to ADWA are strongly associated with the assumption that the transfer is governed by a short range operator. So, it is not obvious that the method remains valid for other weakly bound systems, like ^{11}Be. Even in the case of (d,p) scattering, the transfer matrix element is determined not only by the $n-p$ interaction, but also by the proton-target and neutron target interactions, that define the *remnant* term. It is not clear a-priori the role of these terms, that would have contributions of three-body configurations in which proton and neutron are not so close together.

4.5.2 Continuum Discretized Coupled Channels Born Approximation (CDCC-BA)

In scattering of weakly bound nuclei, coupling to break-up channels can play an important role. DWBA may not be sufficiently accurate, as the three-body wavefunction is not dominated by the elastic channels. ADWA requires to assume the adiabatic approximation

for the composite projectile, which may not be accurate if the collision energy is not sufficiently high. Besides, the simple Johnson-Soper expression requires to assume a short range in the transfer interaction, which may not be accurate beyond (d,p) reactions.

A more accurate approach for transfer is obtained if the three-body wavefunction is approximated in terms of a basis of the states of the relative motion of the $a+v$ sub-system, i.e.

$$\Psi^{(+)}_{\mathbf{K}}(\mathbf{R},\mathbf{r}) \approx \Psi^{\rm CDCC}(\mathbf{R},\mathbf{r}) = \sum_{i=0}^{N} \chi^{(+)}_{\alpha,i}(\mathbf{K}_i,\mathbf{R})\varphi_{av,i}(\mathbf{r}). \tag{4.32}$$

Here, the index i indicates all states explicitly included in a coupled channels calculation $\varphi_{av,i}(\mathbf{r})$, which would correspond in general to a given spin and spin projection ($i=0$ denotes the ground state of the $a+v$ system). This basis of states should include other possible bound states of the $a+v$ system, if present, as well as a suitable discrete representation of the two-body continuum states. In actual calculations, this continuum must be truncated in excitation energy and limited to a finite number of partial waves ℓ associated to the relative co-ordinate $\mathbf{r}$. Normalizable states representing the continuum should be obtained for each ℓ value. This can be achieved making use of a pseudo-state basis and diagonalizing the $a+v$ Hamiltonian [18]. Alternatively, continuum states of the $a+v$ Hamiltonian can be obtained, and normalizable states (bins) can be obtained by averaging these continuum states over a certain energy interval [5].

Once a suitable basis on the $a+v$ co-ordinate is defined, the radial coefficients $\chi^{(+)}_{\alpha,i}(\mathbf{K}_i,\mathbf{R})$ appearing in the expansion (4.32) are obtained as a solution of the set of coupled differential equations:

$$[E-\varepsilon^i_{av}-\hat{T}_\alpha - U^{ii}_{Ab}(\mathbf{R})]\chi^{(+)}_{\alpha,i}(\mathbf{K}_i,\mathbf{R}) = \sum_{j\neq i}^{N} U^{ij}_{Ab}(\mathbf{R})\chi^{(+)}_{\alpha,j}(\mathbf{K}_j,\mathbf{R}), \tag{4.33}$$

where U^{ij}_{Ab} are the transition potentials defined as

$$U^{ij}_{Ab}(\mathbf{R}) = \int d\mathbf{r}\ \varphi^*_{av,i}(\mathbf{r})(U_{ab}+U_{vb})\varphi_{av,j}(\mathbf{r})\,. \tag{4.34}$$

The coupled channels solution $\chi^{(+)}_{\alpha,i}(\mathbf{K},\mathbf{R})$ corresponds to the outgoing waves in all different channels i, for boundary conditions given by a plane wave in the initial bound state $i=0$. The potentials U_{ab} and U_{vb} are to be understood as effective interactions (complex in general) describing the elastic scattering of the corresponding sub-systems, at the same energy per nucleon as in the incident projectile. In particular, U_{vb} will be described in general by a complex optical potential, and will differ from the interaction V_{vb} used to generate the bound state wavefunction of the vb system.

Note that, without any loss of generality, we can introduce an arbitrary auxiliary potential $U_{Ab}(R)$, so that eq.(4.33) can ve written as

$$[E-\varepsilon^i_{av}-\hat{T}_\alpha - U_{Ab}(R)]\chi^{(+)}_{\alpha,i}(\mathbf{K}_i,\mathbf{R}) = \sum_{j}^{N} V^{ij}_{\rm prior}(\mathbf{R})\chi^{(+)}_{\alpha,j}(\mathbf{K}_j,\mathbf{R}), \tag{4.35}$$

where $V^{ij}_{\rm prior}(\mathbf{R})$ are the matrix elements of $V_{\rm prior} = U_{ab} + U_{vb} - U_{Ab}$.

Once the CDCC wavefunction (4.32) is obtained, it can be inserted into Eq. (4.4) to give:

$$\mathcal{T}^{(\rm CDCC)} = \langle \chi^{(-)}_{\beta}(\mathbf{K}', \mathbf{R}')\varphi_{bv}(\mathbf{r}')|V_{\rm post}|\Psi^{\rm CDCC}(\mathbf{R}, \mathbf{r})\rangle. \tag{4.36}$$

with $V_{\rm post} = V_{va} + U_{ab} - U_{aB}$. To clarify the link between the CDCC-BA and DWBA methods it is convenient to rewrite this expression as:

$$\begin{aligned}\mathcal{T}^{(\rm CDCC)} &= \langle \chi^{(-)}_{\beta}(\mathbf{K}', \mathbf{R}')\varphi_{bv}(\mathbf{r}')|V_{\rm post}|\chi^{(+)}_{\alpha,0}(\mathbf{R})\varphi_{av,0}(\mathbf{r})\rangle \\ &+ \sum_{i=1}^{N}\langle \chi^{(-)}_{\beta}(\mathbf{K}', \mathbf{R}')\varphi_{bv}(\mathbf{r}')|V_{\rm post}|\chi^{(+)}_{\alpha,i}(\mathbf{R})\varphi_{av,i}(\mathbf{r})\rangle. \end{aligned}\tag{4.37}$$

The fist term in this expression corresponds to the *direct transfer*, that is, the transfer proceeding directly from the ground state of the projectile (eg. the deuteron, in a (d, p) reaction), whereas the second term accounts for the *multi-step* transfer occurring via the excited states of the projectile ($p - n$ continuum states in the case of the deuteron). These two types of processes correspond, respectively, to the solid and dashed lines in Fig. 4.4(b) for the ^{10}Be(d,p)^{11}Be case. Clearly, the multi-step process going through the breakup channels are omitted in the DWBA calculation. At most, the DWBA considers the effect of these channels on the elastic scattering if a suitable choice of the entrance optical potential is made. The adiabatic approximation includes in principle both mechanisms, but under the assumption that the excited (breakup) channels of the projectile are degenerate with the ground state [Fig. 4.4(c)]. The advantage of the CDCC-BA approach is that all relevant bound and continuum states in the $a+v$ system are explicitly included in the calculation.

Some early comparisons between these three methods can be found in Refs. [24, 15, 2, 18] and the main results are also summarized in Ref. [5]. Due to numerical limitations, these first studies where done using a zero-range approximation of the V_{av} potential. Overall, they find that the ADWA model describes well the direct transfer contribution. However, the multi-step contribution, which are completely absent in DWBA, are described very inaccurately by the adiabatic approximation. At low energies ($E_d < 20$ MeV) the discrepancy between the ADWA and CDCC-BA calculation can be understood because at these energies the adiabatic approximation is questionable. However, even at medium energies ($E_d \approx 80$ MeV) there are situations in which transfer through breakup channels is found to be very significant, and therefore the ADWA method did not work well either. In these situations, the CDCC-BA should be better used instead. The disadvantage of the calculations is that, in principle, a large basis of internal states has to be included, making this approach much more demanding numerically.

Finite-range effects have been studied within the adiabatic approximation in Ref. [20, 22] and were found to be small ($< 10\%$) at energies below 20-30 MeV/u but become more and more important as the incident energy increases. This limitation should be also taken into account in the analysis of experimental data.

4.5.3 The CRC method

It was stated that Eqs. (4.4) and (4.7) provide the exact solution to the 3-body scattering problem, provided that $\Psi^{(+)}_{\mathbf{K}}(\mathbf{R},\mathbf{r})$ (in the post form) or $\Psi^{(-)}_{\mathbf{K}'}(\mathbf{R}',\mathbf{r}')$ (in the prior form) correspond to the exact three-body wavefunctions with the appropriate boundary conditions. However, in practical calculations, these exact solutions are not available and thus they need to be replaced by approximated ones, such as the factorized form used in the DWBA method, the adiabatic wavefunction or the CDCC expansion. In all these approximations, the three-body wavefunction is restricted to configurations corresponding to either the initial or the final channel. For example, in the post representation, the initial state is a solution solution of the three-body Schrödinger equation

$$\left[\hat{T} + V_{av} + V_{vb} + U_{ab} - E\right] \Psi^{(+)}(\mathbf{r},\mathbf{R}) = 0. \tag{4.38}$$

Asymptotically, the solution of this equation is of the form

$$\Psi^{(+)}(\mathbf{r},\mathbf{R}) \to \varphi_{av}(\mathbf{r}) e^{i\mathbf{K}\cdot\mathbf{R}} \; + \; \text{outgoing waves} \tag{4.39}$$

where the "outgoing waves" contain contributions from all open channels. This includes elastic and breakup channels, but also rearrangement channels of the a+b and v+b pairs, if they are present. In principle, the eigenstates of the a+v Hamiltonian form a complete set and hence the expansion Eq. (4.32) should contain all the relevant channels. In particular, the asymptotic part of (4.32) should contain information from all open channels, including rearrangement channels. However, rearrangement channels corresponding to the $v+b$ system would behave asymptotically as a product of the bound wavefunction $\varphi_{vb}(\mathbf{r}'_{vb})$ times a plane wave in the aB co-ordinate. Although these states could be in principle expressed in the $\varphi_{av}(\mathbf{r}_{av})$ basis, this would require require a very large number of energies and angular momenta [5]. In other words, any finite CDCC approximation will describe poorly the contribution from rearrangement channels.

A heuristic way of incorporating rearrangement channels is provided by the Coupled-Reaction-Channels (CRC) framework [23, 19, 26, 29, 12]. We just give a brief outline of the method here, and refer the reader to the referred works for details (see also [1] for a recent review). The idea of the CRC method is to propose a model wavefunction which incorporates explicitly contributions from several mass partitions. For simplicity, let us assume that we wish to consider explicitly excited states (bound or unbound) of the incoming partition plus some excited states of the aB partition. Then, we use the following *ansatz*:

$$\Psi^{(+)}(\mathbf{R},\mathbf{r}) \approx \Psi^{\mathrm{CRC}}(\mathbf{R},\mathbf{r}) = \sum_i \chi^{(+)}_{\alpha,i}(\mathbf{R})\varphi_{av,i}(\mathbf{r}) + \sum_j \chi^{(+)}_{\beta,j}(\mathbf{R}')\varphi_{bv,j}(\mathbf{r}')\,. \tag{4.40}$$

This wavefunction can be interpreted as a generalization of the CDCC expansion of Eq. (4.32). The radial functions $\chi^{(+)}_{\alpha,i}(\mathbf{R})$ and $\chi^{(+)}_{\beta,j}(\mathbf{R}')$ are obtained by substituting the model wavefunction (4.40) into the Schrödinger equation:

$$[H - E]\Psi^{(+)\mathrm{CRC}} = 0. \tag{4.41}$$

To get the equations satisfied by $\chi^{(+)}_{\alpha,i}(\mathbf{R})$ we replace in this equation $\Psi^{\rm CRC}$ by the *ansatz* (4.40), multiply on the left by each of the functions $\varphi^*_{av,i}(\mathbf{r})$ and integrate along $\mathbf{r}$ we get the system of equations:

$$\sum_{i'}\langle\varphi_{av,i}|H-E|\chi^{(+)}_{\alpha,i'}\varphi_{av,i'}\rangle+\sum_{j}\langle\varphi_{av}|H-E|\chi^{(+)}_{\beta,j}\varphi_{bv,j}\rangle=0. \tag{4.42}$$

A complication that arises when solving these equations, is that one have to deal with coupling potentials between internal states $\varphi_{bv,j}$ and $\varphi_{av,i}$ that belong to different Hamiltonians and, therefore, are not mutually orthogonal. These gives rise to the appearance of the so-called non-orthogonality terms in the coupled equations. Furthermore, the coupling potentials are found to be non-local. For all these reasons, the solution of the CRC equations is much more involved than the conventional CC or CDCC equations.

The great advantage of the CRC method is that it can treat transfer couplings beyond the first order (in addition to the inelastic couplings). For example, a possible CRC coupling scheme for our ^{10}Be(d,p)^{11}Be reaction is shown in Fig. 4.4(d).

Appendix A

Rotor and vibrator models

A.1 Axially symmetric particle-rotor model (PRM)

The particle-rotor model (PRM) [7] assumes that the nucleus has a permanent deformation, and hence its radius will not be longer a constant. Instead, the distance from the center to an arbitrary point in the surface characterized by a function of the angles θ' and ϕ'), defined with respect to intrinsic, i.e., *body-fixed*, frame (see Box),

$$r(\theta', \phi') = R_0[1 + \sum_\lambda \beta_\lambda Y_{\lambda 0}(\theta', \phi')] = R_0 + \sum_\lambda \delta_\lambda Y_{\lambda 0}(\theta', \phi')] \equiv R_0 + \Delta(\hat{r}') \tag{A.1}$$

where R_0 is an average radius of the nucleus and hence the remaining term (denoted $\Delta(\theta', \phi')$) represents the deviation of the radius for a particular point on the surface from this average radius. The quantities $\delta_\lambda = \beta_\lambda R_0$ are the *deformation lengths*. The function $\hat{\Delta}(\hat{r}')$ is sometimes referred to as shift-function.

The angular variables in these expressions are referred to the reference frame aligned with the symmetry axis, but can be converted to the laboratory frame (characterized by the variables θ, ϕ) by means of the transformation [see eg. Ref. [8], Eq. (2.24)]:

$$Y_{\lambda 0}(\theta', 0) = \sum_\mu \mathcal{D}^\lambda_{\mu 0}(\omega) Y_{\lambda \mu}(\theta, \phi) \tag{A.2}$$

where $\mathcal{D}$ is the so called *r*otation matrix (or D-matrix) and with $\omega = \{\alpha, \beta, \gamma\}$ are the Euler angles describing the transformation from the body-fixed frame to the laboratory frame. In this particular case (on the three-indexes equal to zero) the D-matrix is just

$$\mathcal{D}^\lambda_{\mu 0}(\alpha, \beta, \gamma) = \sqrt{\frac{4\pi}{2\lambda + 1}} Y_{\lambda \mu}(\theta_0, \phi_0) \tag{A.3}$$

where $\{\theta_0, \phi_0\}$ are the angles defining the orientation of the symmetry axis with respect to the laboratory frame.

The deformation parameter

The deformation parameter, β, measures the departure of a nucleus from the spherical shape. For a spherical nucleus, we have $\beta = 0$. For a nucleus with a quadrupole permanent deformation, we have $\beta_2 \neq 0$. If $\beta_2 > 0$, the nucleus is said to be *prolate* ("rugby ball" shape), whereas for $\beta < 0$ it is said to be *oblate* ("discus-shaped").

Spherical nucleus ($\beta = 0$)

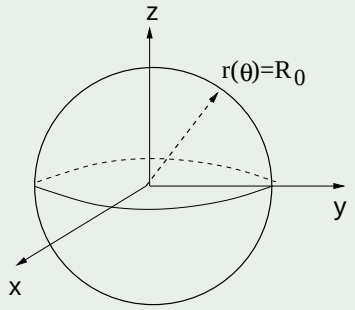

Deformed nucleus ($\beta \neq 0$)

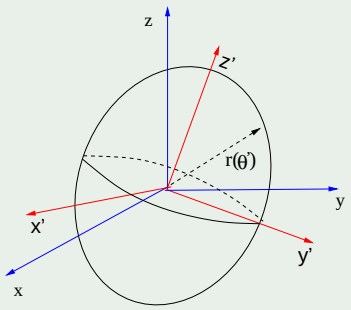

It is convenient to introduce the *deformation length operator*, defined as

$$\hat{\delta}_{\lambda\mu} \equiv \beta_\lambda R_0 \mathcal{D}^\lambda_{\mu 0}(\omega) = \beta_2 R_0 \sqrt{\frac{4\pi}{2\lambda+1}} Y_{\lambda\mu}(\theta_0, \phi_0). \tag{A.4}$$

In terms of this operator, the radius of the nucleus is written in the laboratory frame as

$$r(\theta, \phi) = R_0 + \sum_\mu \hat{\delta}_{\lambda\mu} Y_{\lambda\mu}(\theta, \phi). \tag{A.5}$$

If one assumes that the projectile–target potential is still a function of the distance between the valence particle and the surface of the nucleus, the interaction potential will follow the same functional dependence as $V(r - R_0)$, but replacing R_0 by $r(\theta', \phi')$. Choosing a reference frame with the z axis along the symmetry axis:

$$V^{\rm rot}(\vec{r}, \theta', \phi') = V(r - r(\theta', \phi')). \tag{A.6}$$

This expression is expanded in multipoles as:

$$V^{\rm rot}(r, \hat{r}') = \sum_\lambda V^{\rm rot}_\lambda(r) Y_{\lambda 0}(\hat{r}') \tag{A.7}$$

with

$$V^{\rm rot}_\lambda(r) = 2\pi \int_{-1}^{1} V(r - \hat{\Delta}(\hat{r}')) Y_{\lambda,0}(\theta', 0) d(\cos\theta') \tag{A.8}$$

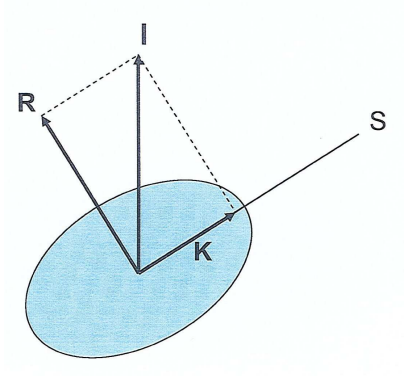

Figure A.1: Angular momenta of a rotor. **I** is the total angular momentum and K its projection along the symmetry axis.

For small deformations, one can perform a Taylor series of the potential (A.6) in powers of Δ:

$$V^{\rm rot}(r,\hat{r}') \approx V^{\rm rot}(r-R_0) - \frac{dV^{\rm coup}}{dr}\sum_{\lambda}\delta_\lambda Y_{\lambda 0}(\hat{r}') \tag{A.9}$$

Inserting this expansion into Eq. (A.8) gives for a multipole $\lambda > 0$

$$V^{\rm rot}_\lambda(r) = -\delta_\lambda \frac{dV^{\rm rot}}{dr} \tag{A.10}$$

Inserting (A.2) into (A.7):

$$V^{\rm rot}(r,\hat{r}') = \sum_{\lambda\mu} V^{\rm rot}_\lambda(r)\mathcal{D}^\lambda_{\mu 0}(\omega)Y_{\lambda\mu}(\hat{r}). \tag{A.11}$$

In the derivation of the DWBA formula for inelastic scattering, we had to evaluate the matrix elements of the deformation length operator between different states of the rotor. These states are also defined in the intrinsic frame and can be characterized by the total angular momentum I and its projection on the symmetry axis, K (see Fig. A.1). These states, denoted $|IK\rangle$, can be transformed to the laboratory frame as[1]

$$|K;IM\rangle = \sqrt{\frac{2I+1}{8\pi^2}}\mathcal{D}^I_{MK}(\omega)|IK\rangle \tag{A.12}$$

The matrix elements thus involve an integral of three D matrices. These are given by (see

[1]This expression is valid for a symmetric rotor. For an asymmetric rigid rotor, there is in general a sum in K, [c.f. Ref. [8], discussion following Eq. (2.21)].

e.g. [8], Appendix V)[2],

$$\int \mathcal{D}^C_{c'c}(\alpha\beta\gamma)\mathcal{D}^A_{a'a}(\alpha\beta\gamma)\mathcal{D}^B_{b'b}(\alpha\beta\gamma)\sin(\beta)d\beta d\alpha d\gamma = (-)^{2B-2A+c+c'}\frac{8\pi^2}{2C+1} \times \langle AaBb|C-c\rangle\langle Aa'Bb'|C-c'\rangle \quad \text{(A.15)}$$

Using this formula, the matrix elements of the transition operator result (I is assumed to be integer here)

$$\langle K; IM|\mathcal{D}^\lambda_{\mu 0}|K; I'M'\rangle = \frac{\sqrt{2I'+1}}{\sqrt{2I+1}}\langle I'M'\lambda\mu|IM\rangle\langle I'K\lambda 0|IK\rangle. \quad \text{(A.16)}$$

Using the Wigner-Eckart theorem (Brink and Satchler convention), the reduced matrix element is

$$\langle K; I\|\mathcal{D}^\lambda\|K; I'\rangle_{\rm BS} = \frac{\sqrt{2I'+1}}{\sqrt{2I+1}}\langle I'K\lambda 0|IK\rangle = (-1)^{I-I'}\langle IK\lambda 0|I'K\rangle. \quad \text{(A.17)}$$

where, in the second equality, we have used the properties of the Clebsch-Gordan coefficients.

A.2 Particle-vibrator model (PVM)

In the PVM model [28], the nucleus is assumed to be spherical, but it can undergo vibrations around the spherical shape. The surface is parametrized as

$$r = R_0[1 + \sum_{\lambda,\mu}\alpha^\dagger_{\alpha\mu}Y_{\lambda\mu}(\hat{r})] \equiv R_0 + \Delta(\hat{r}) \quad \text{(A.18)}$$

with $\Delta(\hat{r}) \equiv \sum_{\lambda\mu}\alpha^\dagger_{\alpha\mu}Y_{\lambda\mu}(\hat{r})$ and where $\alpha_{\lambda\mu}$ are to be understood as dynamical variables, given in terms of phonon creation ($b^\dagger_{\lambda\mu}$) and annihilation ($b_{\lambda\mu}$) operators as:[3]

$$\alpha_{\lambda\mu} = \frac{\beta_\lambda}{\sqrt{2\lambda+1}}[b_{\lambda\mu} + (-1)^\mu b^\dagger_{\lambda,-\mu}] \quad \text{(A.19)}$$

[2] In [8] this expressions is actually given in terms of the 3j symbols

$$\int \mathcal{D}^C_{c'c}(\alpha\beta\gamma)\mathcal{D}^A_{a'a}(\alpha\beta\gamma)\mathcal{D}^B_{b'b}(\alpha\beta\gamma)\sin(\beta)d\beta d\alpha d\gamma = 8\pi^2\begin{pmatrix}A & B & C\\ a & b & c\end{pmatrix}\begin{pmatrix}A & B & C\\ a' & b' & c'\end{pmatrix} \quad \text{(A.13)}$$

Both expressions are simply related taken into account the relation between 3j-symbols and Clebsch-Gordan coefficientes

$$\langle AaBb|C-c\rangle = (-1)^{A-B-c}\sqrt{2C+1}\begin{pmatrix}A & B & C\\ a & b & c\end{pmatrix} \quad \text{(A.14)}$$

[3] Different authors use slightly different definitions of these operators. In any case, for r to be real $\alpha^\dagger_{\alpha\mu}$ must have the same transformation properties as $Y_{\lambda\mu}$, namely, $\alpha^\dagger_{\alpha\mu} = (-1)^\mu\alpha_{\alpha,-\mu}$.

where β_λ is the so-called *zero-point amplitude*, defined as the root mean square of α in the ground state (no phonons) of the system (denote $|0\rangle$):

$$\beta_\lambda^2 = \langle 0| \sum_\mu \alpha_{\lambda\mu}\alpha_{\lambda\mu}^\dagger |0\rangle \tag{A.20}$$

As in the rotational case, one assumes that the projectile–target potential is dependent on the distance of the valence particle to the surface of the deformed nucleus, $V(r,\theta,\varphi) = V^{\rm vib}(r - (R_0 + \Delta(\hat{r}))$. We can expand this interaction in a Taylor series about the equilibrium position of the surface ($R = R_0$)

$$V^{\rm vib}(r - (R_0 + \Delta(\hat{r})) = V(r - R_0) - R_0 \frac{dV^{\rm vib}}{dr}\Delta(\hat{r}) + \ldots \tag{A.21}$$

The states of the nucleus being excited are expressed as $|N; IM\rangle$, where N is the number of phonons of a given multipolarity[4]. The first term in (A.21) cannot alter the number of phonons and hence it has only diagonal matrix elements between nuclear states. The second term, being linear in the amplitude, can connect vibrational states differing by one unit in the number of phonons. For example, for the transition between the ground state of the system for an even nucleus ($N = I = M = 0$) to a one-phonon state of angular momentum I and projection M, we have to evaluate the matrix element

$$\langle 1; IM|\alpha_{\lambda\mu}^\dagger|0; 00\rangle = \frac{\delta_{I,\lambda}\delta_{M,\mu}}{\sqrt{2I+1}}, \tag{A.22}$$

And, for the inverse transition

$$\langle 0; 0\|\alpha_{\lambda\mu}^\dagger\|1; M\rangle = (-1)^I \delta_{I,\lambda}\delta_{M,\mu}. \tag{A.23}$$

Of course, for the diagonal terms we have

$$\langle 1; 1\|\alpha_{\lambda\mu}^\dagger\|1; I\rangle = \langle 0; 0\|\alpha_{\lambda\mu}^\dagger\|0; 0\rangle = 0. \tag{A.24}$$

[4]A generic vibrational mode might contain phonons of different multipolarities. However, we will consider only states containing phonons of a given multipolarity.

Appendix B

Wigner-Eckart theorem and reduced matrix elements

The Wigner-Eckart theorem establishes that the matrix element of a tensor operator $\hat{O}_{\lambda\mu}$ can be expressed as

$$\langle I_f M_f|\hat{O}_{\lambda\mu}|I_i M_i\rangle = C(I_i, I_f, \lambda)\langle I_f M_f|\lambda\mu I_i M_i\rangle\langle I_f\|\hat{O}_\lambda\|I_i\rangle \tag{B.1}$$

where the object $\langle I_f\|\hat{O}_\lambda\|I_i\rangle$ is the so called *reduced matrix element*, and is independent onf the value of the z projections. The coefficient $C(I_i, I_f, \lambda)$ is an arbitrary function of I_i, I_f, and λ, but is independent of the projections. Several conventions are encountered in the literature, giving rise to different definitions for the reduced matrix elements (and to the unavoidable confusion when works using different conventions are to be compared!). Here, we cite two popular conventions followed in Nuclear Physics:

1. Bohr-Mottelson (BM) convention: $C(I_i, I_f, \lambda) = (2I_f + 1)^{-1/2}$. Hence,

$$\langle I_f M_f|\hat{O}_{\lambda\mu}|I_i M_i\rangle = (2I_f + 1)^{-1/2}\langle I_f M_f|\lambda\mu I_i M_i\rangle\langle I_f\|\hat{O}_\lambda\|I_i\rangle_{\mathrm{BM}} \tag{B.2}$$

2. Brink-Satchler (BS) convention: $C(I_i, I_f, \lambda) = (-1)^{2\lambda}$

$$\langle I_f M_f|\hat{O}_{\lambda\mu}|I_i M_i\rangle = (-1)^{2\lambda}\langle I_f M_f|\lambda\mu I_i M_i\rangle\langle I_f\|\hat{O}_\lambda\|I_i\rangle_{\mathrm{BS}} \tag{B.3}$$

So, these reduced matrix elements will be related by:

$$\langle I_f\|\hat{O}_\lambda\|I_i\rangle_{\mathrm{BM}} = \sqrt{2I_f + 1}\langle I_f\|\hat{O}_\lambda\|I_i\rangle_{\mathrm{BS}} \tag{B.4}$$

Bibliography

[1]

[2] H. Amakawa and N. Austern. Adiabatic-approximation survey of breakup effects in deuteron-induced reactions. *Phys. Rev. C*, 27:922, 1983.

[3] H. Amakawa, S. Yamaji, A. Mori, and K. Yazaki. Adiabatic Treatment of Elastic Deuteron-Nucleus Scattering. *Phys. Lett.*, 82B:13, 1979.

[4] H. Amakawa and K. Yazaki. Adiabatic treatment of deuteron break-up on a nucleus. *Phys. Lett.*, 87B:159, 1979.

[5] N. Austern, Y. Iseri, M. Kamimura, M. Kawai, G. Rawitscher, and M. Yahiro. *Phys. Rep.* **154**, *125*, (1987).

[6] Norman Austern. *Direct nuclear reaction theories.* Wiley-Interscience New York, 1970.

[7] A. Bohr and B. Mottelson. *Nuclear Structure.* New York, W. A. Benjamin edition, 1969.

[8] D.M. Brink and G.R. Satchler. *Angular momentum.* Clarendon Press, 1994.

[9] Herman Feshbach. A unified theory of nuclear reactions. i. *Annals of Physics*, 5(2):357, 1958.

[10] Herman Feshbach. A unified theory of nuclear reactions. ii. *Annals of Physics*, 19(2):287–313, 1962.

[11] Norman K. Glendenning. *Direct Nuclear Reactions.* Academic Press, Inc., 1983.

[12] Norman K Glendenning. *Direct nuclear reactions.* World scientific, 2004.

[13] J.D. Harvey and R.C. Johnson. *Phys. Rev.* **C3**, *636*, (1971).

[14] D. Hasselgren, P.U. Renberg, O. Sundberg, and G. Tibell. Inelastic scattering of 185 MeV protons from light nuclei. *Nuclear Physics*, 69(1):81 – 102, 1965.

[15] Yasunori Iseri, Masanobu Yahiro, and Masahiro Nakano. Investigation of Adiabatic Approximation of Deuteron-Breakup Effect on (d, p) Reactions. *Progress of Theoretical Physics*, 69:1038, 1983.

[16] R. C. Johnson and P. J. R. Soper. Contribution of deuteron breakup channels to deuteron stripping and elastic scattering. *Phys. Rev. C*, 1:976, 1970.

[17] R. C. Johnson and P. C. Tandy. An approximate three-body theory of deuteron stripping. *Nucl. Phys. A*, 235:56, 1974.

[18] Mitsuji Kawai. Chapter II. Formalism of the Method of Coupled Discretized Continuum Channels. *Progress of Theoretical Physics Supplement*, 89(Supplement 1):11, 1986.

[19] Mitsuji Kawai, Masayasu Kamimura, and Kazuo Takesako. Chapter V. Coupled-Channels Variational Method for Nuclear Breakup and Rearrangement Processes. *Progress of Theoretical Physics Supplement*, 89(Supplement 1):118, 1986.

[20] A. Laid, J.A. Tostevin, and R.C. Johnson. *Phys. Rev.* **C48**, *1397*, (1993).

[21] A. Messiah. *Quantum Mechanics*. Number v. 2 in Quantum Mechanics. North-Holland, 1981.

[22] N. B. Nguyen, F. M. Nunes, and R. C. Johnson. Finite-range effects in (d, p) reactions. *Phys. Rev. C*, 82:014611, 2010.

[23] Takashi Ohmura, Bunryu Imanishi, Munetake Ichimura, and Mitsuji Kawai. Study of Deuteron Stripping Reaction by Coupled Channel Theory. II Properties of Interaction Kernel and Method of Numerical Solution. *Progress of Theoretical Physics*, 43:347, 1970.

[24] George H. Rawitscher. Effect of deuteron breakup on $(d,\ p)$ cross sections. *Phys. Rev. C*, 11:1152, 1975.

[25] G. R. Satchler. Adiabatic Deuteron Model and the ^{208}Pb(p, d) Reaction at 22 MeV. *Phys. Rev. C*, 4:1485, 1971.

[26] G.R. Satchler. *Direct Nuclear Reactions*. Oxford University Press, New York, (1983).

[27] M. J. Smithson, J. S. Lilley, M. A. Nagarajan, P. V. Drumm, R. A. Cunningham, B. R. Fulton, and I. J. Thompson. The Threshold Anomaly in Inelastic Scattering. *Nucl.Phys.*, A517:193, 1990.

[28] Taro Tamura. Analyses of the scattering of nuclear particles by collective nuclei in terms of the coupled-channel calculation. *Rev. Mod. Phys.*, 37:679, 1965.

[29] Ian J Thompson and Filomena M Nunes. Nuclear reactions for astrophysics. *Nuclear Reactions for Astrophysics, by Ian J. Thompson, Filomena M. Nunes, Cambridge, UK: Cambridge University Press, 2009*, 1, 2009.

[30] G. L. Wales and R. C. Johnson. Deuteron break-up effects in (p, d) reactions at 65 MeV. *Nucl. Phys. A*, 274:168, 1976.